

**THE EFFECTS OF CORROSION IN
REINFORCED CONCRETE WITH ADDITION OF STEEL
FIBER AND MINERAL ADMIXTURE**

A Thesis

submitted in partial fulfillment of the requirements for the award of the degree

of

MASTER OF TECHNOLOGY

IN

CIVIL ENGINEERING

With specialization in

STRUCTURAL ENGINEERING

*Under the
supervision of*

**DR. SAURAV
(ASSISTANT PROFESSOR)**

by

**NIMISHA SHARMA
(162654)**



Education • Enlightenment • Empowerment

JAYPEE UNIVERSITY OF INFORMATION TECHNOLOGY,

WAKNAGHAT, SOLAN- 173234

HIMACHAL PRADESH, INDIA

(MAY-2018)

CERTIFICATE

This is to certify that the work which is being presented in the thesis titled “ THE EFFECTS OF CORROSION IN REINFORCED CONCRETE WITH ADDITION OF STEEL FIBER AND MINERAL ADMIXTURE” in partial fulfillment of the requirements for the award of the degree of Master of Technology in Civil Engineering with specialization in “Structural Engineering” and submitted to the Department of Civil Engineering, Jaypee University of Information Technology, Wagnaghat is an authentic record of work carried out by Nimisha Sharma (162654) during a period from July 2017 to May 2018 under the supervision of Dr. Saurav (Assistant Professor), Department of Civil Engineering, Jaypee University of Information Technology, Wagnaghat.

The above statement made is correct to the best of our knowledge.

Date:

Dr. Ashok Kumar Gupta
Professor & Head of Department
Department of Civil Engineering
JUIT, Wagnaghat

Dr. Saurav
Assistant Professor
Department of Civil Engineering
JUIT, Wagnaghat

External Examiner

ACKNOWLEDGEMENT

The success and outcome of this project required a lot of guidance and assistance from many people and I am extremely privileged to have this all along the completion of my project. All that I have done is only due to such supervision and assistance and I would not forget to thank them. I respect and thank **Dr. Saurav** for providing me an opportunity to do the project work under his constant supervision as well as for providing necessary information regarding the project. I am extremely thankful to him for providing such a nice support and guidance, although he had busy schedule.

I express deep appreciation and sincere thanks to **Dr. Ashok Kumar Gupta**, Professor and Head of the Civil Engineering Department for providing all kind of possible help and encouragement during project work.

I owe my deep gratitude to Mr. Itesh Singh, who helped me during the project work and guided us all along in the experimental work performed in the concrete laboratory, until the completion of my project work.

I would thank the almighty for empowering me to work fully on my project and last but not the least like to thank my parents for their continuous support and motivation.

Finally, I would like to thank to all who directly or indirectly helped me.

ABSTRACT

As soon as the metal is extracted from their ores (Unstable), the reverse process begins, i.e., nature tries to convert them back into the form in which they were (Stable). This is due to attack of the gases present in the atmosphere on the surface of the metal converting it into compounds such as oxides, sulphides, carbonates, sulphates etc. the most common example of corrosion is rusting of iron. Rust is hydrated ferric oxide ($\text{Fe}_2\text{O}_3 \cdot \text{XH}_2\text{O}$). Some other examples are tarnishing of silver, developing of green coating on copper and bronze. Rusting of steel is of our main concern as its usage in civil engineering industry is very important. Specifically in reinforced concrete, despite all the information available on the topic, corrosion of steel continues to be a problem faced by many engineers and prevention of corrosion still requires considerable effort. The ageing transportation infrastructure and the high cost associated with extensive repair or replacement of many structures presents an engineering challenge. In this study extensive literature survey is carried out in which focus was mostly confined to corrosion induced by accelerated corrosion method. Following report shows a comparison among various reinforced concrete mixes after corrosion. A simple reinforced concrete specimen, reinforced concrete mixed with steel fiber specimen and reinforced concrete mixed with steel fiber and ultra-fine slag specimen were made by varying clear cover and reinforcement diameter. To corrode by using accelerated corrosion method and were compared for corrosion by degree of induced corrosion, flexural strength before and after corrosion and corrosion penetration depth.

Key words: *Corrosion, Accelerated Corrosion, Impressed Current Method, Corrosion Depth, Degree of Induced Corrosion, Ultra-fine Slag, Steel Fiber, Faraday's Law.*

TABLE OF CONTENT

	Page No.
CERTIFICATE	ii
ACKNOWLEDGEMENT	iii
ABSTRACT	iv
LIST OF ABBREVIATIONS	ix
LIST OF FIGURES	x
LIST OF TABLES	xii
1 CHAPTER 1 : INTRODUCTION	1-13
1.1 GENERAL	1
1.2 ELECTROCHEMISTRY INVOLVED IN CORROSION	2
1.2.1 THERMODYNAMICS	2
1.2.2 NERNST EQUATION	3
1.2.3 POURBAIX DIAGRAM	4
1.2.3.1 POURBAIX DIAGRAM FOR WATER	4
1.2.3.2 POURBAIX DIAGRAM FOR IRON WATER SYSTEM	5
1.3 CAUSES OF CORROSION IN CONCRETE	6
1.3.1 CARBONATION OF CONCRETE	6
1.3.2 CHLORIDE INGRESS IN CONCRETE	7
1.4 CORROSION OF STEEL IN CONCRETE	7
1.5 ELECTROCHEMICAL TECHNIQUES USED FOR CORROSION DETERMINATION	8
1.5.1 HALF CELL POTENTIAL TECHNIQUE	8
1.5.2 LINEAR POLARIZATION RESISTANCE	9
1.5.3 ELECTROCHEMICAL IMPEDANCE SPECTROSCOPY	9
1.5.4 POTENTIODYNAMIC CYCLIC POLARIZATION	9
1.5.5 GALVANO-DYNAMIC POLARIZATION	9
1.5.6 GRAVIMETRY	9
1.6 ACCELERATED CORROSION TESTING	10

1.6.1	ARTIFICIAL CLIMATE TECHNIQUE	11
1.6.2	IMPRESSED CURRENT TECHNIQUE/ GALVANOSTATIC METHOD	11
2	CHAPTER 2 : LITERATURE REVIEW	14-28
2.1	GENERAL	14
2.2	EFFECTIVENESS OF IMPRESSED CURRENT TECHNIQUE TO STIMULATE CORROSION OF STEEL REINFORCEMENT IN CONCRETE.	14
2.3	EFFECTS OF RUST AND SCALE OF REINFORCING BARS ON THE BOND PERFORMANCE OF REINFORCEMENT CONCRETE	15
2.4	ADVANCED METHODS OF CORROSION MONITORING	16
2.5	LABORATORY SIMULATION OF CORROSION DAMAGE IN REINFORCED CONCRETE	16
2.6	EXPERIMENTAL AND NUMERICAL INVESTIGATION OF CORROSION-INDUCED COVER CRACKING IN REINFORCED CONCRETE STRUCTURES	17
2.7	ESTIMATING CRITICAL CORROSION FOR INITIATION OF LONGITUDINAL CRACKS IN RC STRUCTURES CONSIDERING PHASES AND COMPOSITION OF CORROSION PRODUCTS	17
2.8	EVALUATION OF THE MECHANICAL PROPERTIES OF STEEL REINFORCEMENT EMBEDDED IN CONCRETE SPECIMEN AS A FUNCTION OF THE DEGREE OF REINFORCEMENT CORROSION	18
2.9	A MODEL FOR PREDICTING TIME TO CORROSION-INDUCED COVER CRACKING IN REINFORCED CONCRETE STRUCTURES	18
2.10	MODELING CORROSION-INDUCED CRACKING IN REINFORCED CONCRETE	20

2.11	FACTORS CONTROLLING CRACKING OF CONCRETE AFFECTED BY REINFORCEMENT CORROSION	20
2.12	ANALYSIS ON COMPRESSIVE STRENGTH OF CONCRETE WITH PARTIAL REPLACEMENT OF CEMENT WITH ALCCOFINE	21
2.13	A STUDY ON CORROSION OF REINFORCEMENT IN CONCRETE AND EFFECT OF INHIBITOR ON SERVICE LIFE OF RCC	21
2.14	STEEL FIBER REINFORCED CONCRETE	22
2.15	RESEARCH GAP	23
2.16	RESEARCH OBJECTIVES	23
3	CHAPTER 3: EXPERIMENTAL INVESTIGATIONS	24-40
3.1	GENERAL	24
3.2	MATERIAL USED	24
3.2.1	AGGREGATES	24
3.2.2	BINDER	26
3.2.2.1	PORTLAND POZZOLANA CEMENT	26
3.2.2.2	ALCCOFINE	27
3.2.3	STEEL FIBER	28
3.2.4	WATER	29
3.3	TESTING OF MATERIALS	30
3.3.1	CEMENT	30
3.3.1.1	STANDARD CONSISTENCY	30
3.3.1.2	INITIAL SETTING TIME	31
3.3.1.3	FINAL SETTING TIME	31
3.3.1.4	SPECIFIC GRAVITY	31
3.3.1.5	COMPRESSIVE STRENGTH	32
3.3.1.6	TENSILE STRENGTH	32
3.3.2	SAND	33
3.3.2.1	SPECIFIC GRAVITY	33

3.3.2.2	GRADING OF FINE AGGREGATES	33
3.3.3	COARSE AGGREGATES	34
3.3.3.1	WATER ABSORPTION	34
3.3.3.2	SPECIFIC GRAVITY	35
3.4	MIX DESIGN	35
3.4.1	DESIGN SPECIFICATION	36
3.4.2	TEST DATA FOR MATERIALS	36
3.5	BATCHING, MIXING AND CASTING OF SPECIMENS	36
3.6	PROCESSING IMPRESSED CURRENT METHOD	39
3.6.1	SET-UP USED FOR INDUCING REINFORCEMENT CORROSION THROUGH IMPRESSED CURRENT	39
4	CHAPTER 4 : RESULT AND DISCUSSION	41-51
4.1	GENERAL	41
4.2	CALCULATIONS AND RESULTS	41
4.2.1	DEGREE OF INDUCED CORROSION	41
4.2.2	CALCULATION OF INDUCED CORROSION	42
4.2.3	COMPARSION OF ACTUAL MASS LOSS AND THEORETICAL MASS LOSS	43
4.2.4	EFFECT OF COVER DEPTH ON ACTUAL MASS LOSS	45
4.2.5	FLEXURAL STRENGTH OF CORRODED AND NON CORRODED SAMPLES	47
4.2.6	DEPTH OF PENETRATION OF CORROSION	49
5	CHAPTER 5: CONCLUSION AND RECOMMENDATIONS	52-52
5.1	CONCLUSION	52
5.2	FUTURE SCOPE	52
	REFERENCES	53-57

LIST OF ABBREVIATION

SCE	Saturated Calomel Electrode
OCPT	Open Circuit Potential Technique
LPR	Linear Polarization Resistance
SP	Surface Potential
AE	Acoustic Emission
FO	Fiber Optic
POTs	Potentiometer displacement Transducers

LIST OF FIGURES

Figure No.	Caption	Page No.
1.1	Activation Complex, showing transfer of ions into solution	2
1.2	Pourbaix diagram for water at 25 ° C	4
1.3	Pourbaix diagram for the iron – water system at 25 ° C	5
1.4	The cathodic, anodic, oxidation and hydration reaction for corroding steel	8
1.5	Corrosion model	11
1.6	Schematic of Galvanostatic technique to induce corrosion	12
1.7	Accelerated corrosion test setup	12
1.8	Arrangement of Accelerated Corrosion	13
2.1	Effect of corrosion level on the bond strength of steel bars	15
2.2	Relationship between time to cover cracking and cover thickness	19
2.3	Relationship between time to cover cracking and steel diameter	19
2.4	Relationship between time to cover cracking and tensile strength of concrete	19
2.5	Relationship between time to cover cracking and volume expansive ratio	19
2.6	Specimen 1	20
2.7	Specimen 2	20
2.8	Compressive strength of concrete with various % of alccofine for 7 days curing	21
2.9	Compressive strength of concrete with various % of alccofine for 28 days curing	21
2.10	The stages of rebar corrosion	22
3.1	IS sieves for sieve analysis	26
3.2	Pozzolana Portland cement	27
3.3	Ultra-fine slag	28
3.4	Steel fiber	29

3.5	Schematic representation of insufficient, sufficient and excess water for hydration	30
3.6	Standard Consistency	30
3.7	Compressive test on cement	32
3.8	Preparation of moulds	38
3.9	Random mixing of steel fiber	38
3.10	Casting of samples	39
3.11	Curing of samples	39
3.12	DC voltage source	40
3.13	Impressed current setup	40
4.1	Corroded reinforcement	42
4.2	Comparison of Actual mass loss and Theoretical mass loss	44
4.3	Variation of Actual mass (M_{ac}) for different cover depths in RCC beams	45
4.4	Staining due to steel fiber corrosion	46
4.5	Variation of Actual mass (M_{ac}) for different cover depths in Steel fiber reinforced concrete beams	46
4.6	Variation of Actual mass (M_{ac}) for different cover depths in Steel fiber reinforced concrete along with ultra-fine slag beams	47
4.7	Flexure testing of corroded samples	48
4.8	Comparison of flexure strength of corroded and non-corroded specimen	49
4.9	Corrosion depth of the concrete samples	51

LIST OF TABLES

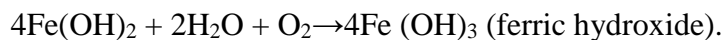
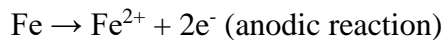
Table No.	Caption	PAGE No.
3.1	Classification of fine aggregates based on FM	26
3.2	Physical and chemical properties of alccofine	28
3.3	Properties of used steel fiber	29
3.4	Grading of sand on particle basis	33
3.5	Sieve analysis of fine aggregates with weight of sample = 1000g, we get a zone 4 fine aggregate	34
4.6	Specimen Classification	38
4.1	Calculation of Degree of induced corrosion	43
4.2	Comparison of actual mass loss (M_{ac}) of steel bars with the theoretical mass loss (M_{th}).	44
4.3	Comparison of flexural strength of corrode and non-corroded bars.	48
4.4	Depth of penetration of corrosion in the concrete samples	50

CHAPTER 1

INTRODUCTION

1.1 GENERAL

The alkaline nature of calcium hydroxide with a pH of about 13 prevents the corrosion of the steel reinforcement by forming a thin protective layer of iron oxide on the surface known as passivity. If the concrete is permeable, then carbonation spreads to the concrete in contact with the steel or soluble chlorides can penetrate up to the reinforcement and if water and oxygen are present, then corrosion of reinforcement takes place. The passive iron oxide layer destroys when the pH falls below about 11.0 and carbonation lowers the pH to about 9. The formation of rust results in an increase in volume compared with the original steel so that swelling pressures will cause cracking and spalling of the concrete. Corrosion of steel occurs because of electrochemical reaction, when two dissimilar metals are electrically connected in the presence of moisture and oxygen. This same process takes place in steel alone because of differences in the electro-chemical potential on the surface, which forms anodic and cathodic regions, connected by the electrolyte in the form of the salt solution in the hydrated cement. The positively charged ferrous ions Fe^{2+} at the anode pass into solution while the negatively charged free electrons e^- pass along the steel into the cathode where they are absorbed by the components of the electrolyte and combine with water and oxygen to form hydroxyl ions $(\text{OH})^-$. Then hydroxyl ions combine with the ferrous ions to form ferric hydroxide and this is then, converted to rust by further oxidation. Thus, we can write:



We see that water regenerates and is needed only for the continuation of process whereas the oxygen is consumed. Thus, there is no corrosion in a completely dry atmosphere, probably below a relative humidity of 40 per cent.

1.2 ELECTROCHEMISTRY INVOLVED IN CORROSION

1.2.1 Thermodynamics

The iron is present in the form of oxides in natural environment. When thermal or mechanical processes are applied to convert iron into pure steel, it becomes thermodynamically unstable, and always tends to revert to its original form, which is at a lower level of energy, i.e. in the form of oxides. Hence, the steel always tends to corrode to form oxides in an environment where humidity and oxygen are present.

Thermodynamic describes the existence of any chemical reaction. The inclination of a chemical reaction to go forward is determined by the change in Gibbs free energy Δ of a system. When a metal dipped into a solution which contains the ions of same metal, the metal ions start following into the solution. Each metallic atom is considered as an ion containing some amount of energy level that can be denoted by its chemical Gibbs free energy (Figure 1.1). Due to thermal agitation, metal ions tend to jump into solution by crossing the energy barrier which forms the breakage of their electronic bonds. The difference between highest energy level and G_r represents the energy of activation ΔG^\ddagger (E_a), which is required for the transition of metal into the solution.

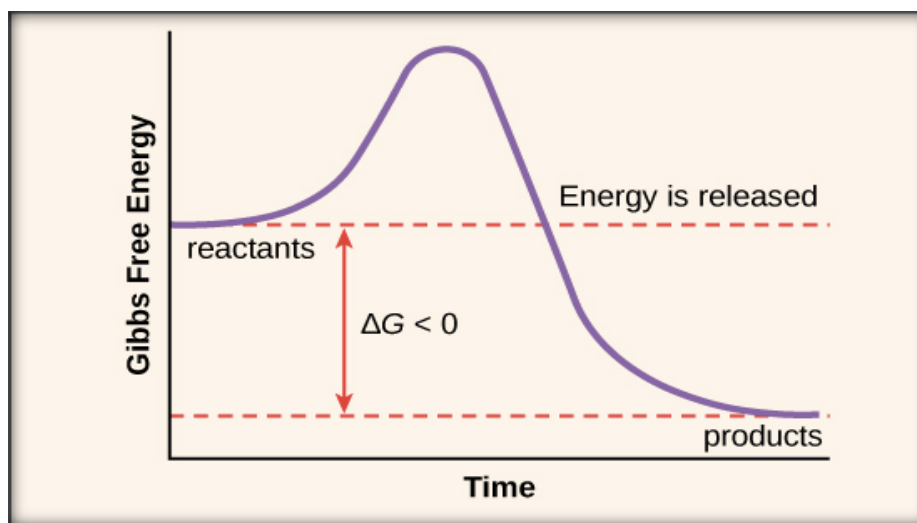
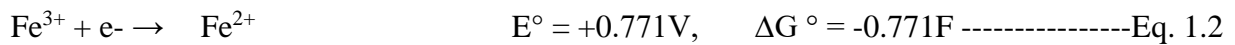
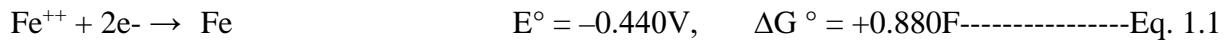


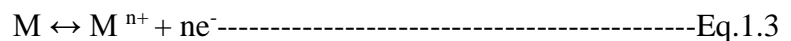
Figure 1.1: Activation Complex, showing transfer of ions into solution. [51]

The Eq. 1.1 and Eq. 1.2 are examples of iron dissolution and conversion of ferric ions into ferrous ions. More negative value of Gibbs free energy shows more rapid forward reaction, so in Eq. 1.2, the reaction will go forward, but in first reaction, it would not proceed forward naturally [51].



1.2.2 Nernst Equation

Nernst established an equation to calculate the potential of an electrochemical reaction. The reaction depends upon the activities of reactant and products. When a metal is dipped into a solution, metal ions starts moving into solution due to potential difference, however the presence of positive ions near the metal-water interface and excess of electrons at the metal surface create a potential barrier and halts the further dissolution of metal ions.



This creates a dynamic equilibrium this which corresponds to a potential E, that represent the potential between the metal M and solution containing ion Mⁿ⁺. Reversible electrode potential designated as E_{rev}. When this equilibrium is formed, there is equality between the change in Gibbs free energy ΔG_{c,r} of the dissolution reaction and electrical energy W_E needs to cross the potential barrier .

For an electrochemical reaction electrical energy is written in absolute term of the following equation [51]:

$$W_E = \eta F E \text{-----Eq.1.4}$$

Where, F = Faraday number

The thermodynamic relation between standard Gibbs free ΔG[°] and Gibbs free energy at any instance is given as

$$\Delta G = \Delta G^\circ + RT \ln K \text{-----Eq.1.5}$$

Where: R is the gas constant, 8.314 J/ mol. k, T is the temperature, K is the rate of reaction.

Since,
$$\Delta G^\circ = - \eta F E^\circ \text{-----Eq.1.6}$$

E[°] is standard electrode potential and is η number of electrons taking part in a reaction. The general equation can be written as,

$$\Delta G = - \eta F E$$

$$- \eta F E = - \eta F E^\circ + RT \ln K$$

$$E = E^\circ - \frac{RT}{nF} \ln K \text{-----Eq.1.7}$$

Eq. 1.7 is Nernst equation which gives the instantaneous potential of an electrochemical cell in terms of reaction rate K, which in turn related to the activities of products and reactants.

1.2.3 Pourbaix Diagram

A concept of thermodynamics data in the form of potential-pH diagram, which relates to electrochemical and corrosion behavior of any metal in water. These diagrams display at a glance the exact condition of potential and pH under which the metal either does not react or reacts to form specific oxides or complex ions, i.e. the Pourbaix diagram shows the potential and pH domains in which a metal is stable. A particular diagram is called “the Pourbaix diagram for the iron-water system”, “the Pourbaix diagram for the zinc-water system,” etc. They are examples of predominance area diagrams. The objective is to represent the comparative stabilities of solid phases and soluble ions that were produced by reaction between a metal and an aqueous atmosphere as functions of two parameters, the electrode potential, E, and the pH of the environment.

1.2.3.1 Pourbaix diagram for water

Each line of a Pourbaix diagram represents conditions of thermodynamic equilibrium for some reaction. The Pourbaix diagram for water is presented in Figure 1.2. Above line *b*, oxygen is evolved in accord with the reaction $\text{H}_2\text{O} \rightarrow \frac{1}{2}\text{O}_2 + 2\text{H}^+ + 2e^-$. For this equilibrium, the relationship between potential and pH is, from the Nernst equation,

$$\phi = \phi^\circ - 2.303 \frac{RT}{nF} \log_e \frac{1}{(\text{H}^+)^2}$$

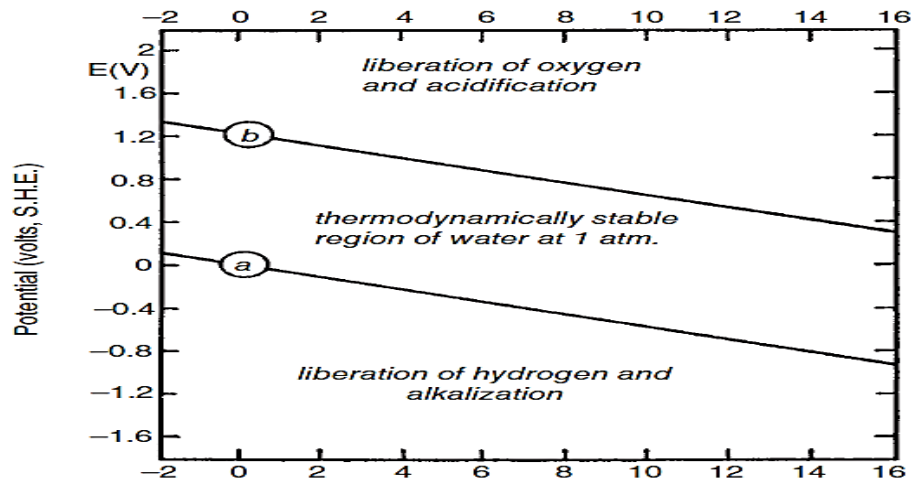


Figure 1.2 : Pourbaix diagram for water at 25 ° C, showing the oxygen line, *b* , above which oxygen is evolved, and hydrogen line, *a* , below which hydrogen is evolved, from the surface of an immersed electrode. Between these two lines, water is stable. [48]

With $\phi^\circ = 1.229$, $T = 298.2$ K, $R = 8.314$ J/deg- mole, and $F = 96,500$ C/eq

We have, $\phi = 1.229 - 0.0592 \text{ pH}$

Above line *b*, defined by this equation, oxygen was evolved at the surface of an immersed electrode. Below this line, water is stable. Below line *a*, hydrogen was evolved in accord with the reaction

$2\text{H}^+ + 2e^- \rightarrow \text{H}_2$. By using the Nernst equation for this equilibrium, we get have

With $\phi^\circ = 0$, $\phi = -0.0592 \text{ pH}$

1.2.3.2 Pourbaix diagram for iron water system

A horizontal line represents a reaction that does not involve pH that is, neither H^+ nor OH^- is involved, as in the reaction, $\text{Fe}^{2+} + 2e^- \rightarrow 2\text{Fe}$. For this equilibrium, using the Nernst equation, (Eq. 1.7) we obtain:

$$\phi = \phi^\circ - 2.303 \frac{RT}{nF} \log_e \frac{1}{(\text{Fe}^{2+})}$$

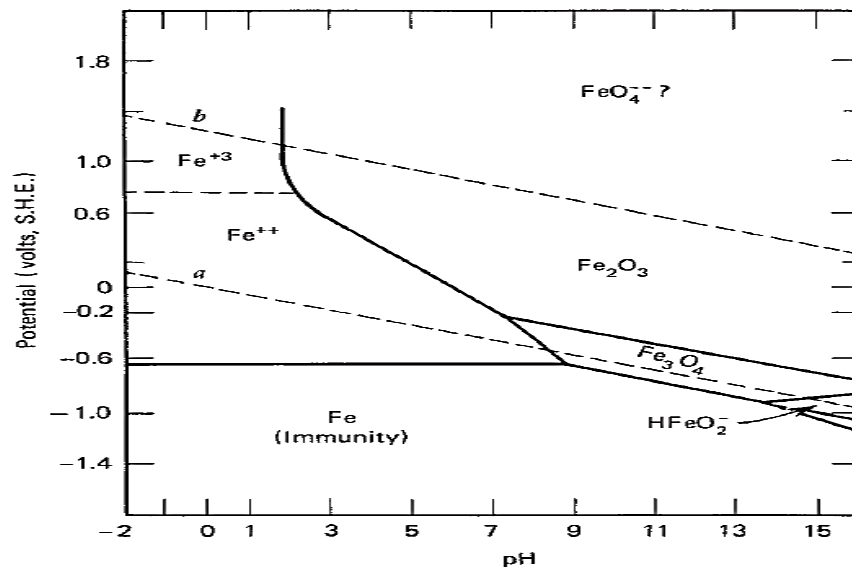


Figure 1.3: Pourbaix diagram for the iron – water system at 25°C, considering Fe, Fe_3O_4 , and Fe_2O_3 as the only solid substances[48].

$$\phi = -0.440 + 0.0296 \log (\text{Fe}^{2+})$$

If (Fe^{2+}) is taken as 10^{-6} , then $\phi = -0.617 \text{ V}$, a horizontal line on the Pourbaix diagram.

A vertical line involves H^+ or OH^- , but not electrons. The vertical line at pH 1.76 represents the equilibrium reaction, $2\text{Fe}^{3+} + 3\text{H}_2\text{O} \rightarrow \text{Fe}_2\text{O}_3 + 6\text{H}^+$. To the right of this line (i.e., at $\text{pH} > 1.76$), Fe_2O_3 is the stable phase and this oxide, as a protective film, would be expected to provide some protection against corrosion. To the left of this line (i.e., at $\text{pH} < 1.76$), ferric ions in solution are stable, and corrosion is expected to take place without any protection afforded by a surface oxide film.

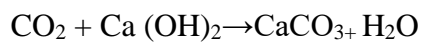
A sloping line involves H^+ , OH^- and electrons. $Fe_2O_3 + 6H^+ + 2e^- \rightarrow 2Fe^{2+} + 3H_2O$. To the right of this line, Fe_2O_3 is a stable phase that forms a surface oxide film that protects the underlying metal from corrosion. To the left of this line, Fe^{2+} is a stable species in solution.

The pH values in Pourbaix diagrams are those of solution in immediate contact with the metal surface. The fields marked Fe_2O_3 and Fe_3O_4 are sometimes labeled “passivation” on the assumption that iron reacts in these regions to form protective oxide films. This is correct only insofar as passivity accounted for by a diffusion – barrier oxide layer.

1.3 CAUSES OF CORROSION IN CONCRETE

1.3.1 Carbonation of Concrete

Carbonation is the result of the interaction of carbon dioxide gas in the atmosphere with the alkaline hydroxides in the concrete. Like many other gases carbon dioxide dissolved in water to form an acid. Unlike most other acids, the carbonic acid does not attack the cement paste, but just neutralizes the alkalis in the pore water, mainly forming calcium carbonate that lies in the pores.



Normally there is a lot of calcium hydroxide in the concrete pores than can be dissolved in the pore water. This helps maintain the pH at its usual level of around 12 or 13 as the carbonation reaction occurs. However, eventually all the locally available calcium hydroxide ($Ca(OH)_2$) reacts, precipitating the calcium carbonate and allowing the pH to fall to a level where steel will corrode [44]. The carbonation can occur even when the concrete cover depth to the reinforcing steel is high. This may be due to a very open pore structure where pores are well connected together and allow rapid CO_2 ingress. It may also happen when alkaline reserves in content, high water cement ratio and poor curing of the concrete.

Carbonation depth is the average distance, from the surface of concrete or mortar where the carbon dioxide has reduced the alkalinity of the hydrated cement [21]. A carbonation front proceeds into the concrete following the laws of diffusion [48]. The carbonation depth is considered dependent on square root of time, and a coefficient that takes account of the concrete conditions.

$$x = K\sqrt{t}$$

Where: x =carbonation depth, t =time and K is the diffusion coefficient.

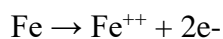
K depends upon the concrete quality, temperature, RH% and the CO₂ concentration around concrete. Depending on the concrete quality and curing condition, the carbonation depth is different. The depth of carbonation can be determined by different techniques. As carbonation reduces the pH, therefore determination pH of concrete by applying pH indicators such as phenolphthalein to a freshly fractured or freshly cut surface of concrete can be used to estimate the depth of carbonation. Upon application of phenolphthalein, noncarbonated areas turn red or purple while carbonated areas remain colorless. Maximum color change to deep purplish red occurs at pH of 9.8 or higher. Below 9.8 the color may be pink and at pH of 8 colorless.

1.3.2 Chloride ingress in concrete

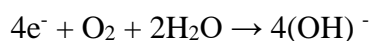
Chloride ions can be present in the concrete due to the use of chloride contaminated components or the use of 9091 as an accelerator when mixing the concrete, or by diffusion into the concrete from the outside environment [48]. A localized breakdown of the passive layer occurs when sufficient amount of chlorides reach reinforcing bars, and the corrosion process is then initiated. Chlorides in concrete can be either dissolved in the pore solution (free chlorides) or chemically and physically bound to the cement hydrates and their surfaces (bound chlorides). Only the free chlorides dissolved in the pore solution are responsible for initiating the process of corrosion.

1.4 CORROSION OF STEEL IN CONCRETE

Corrosion in concrete is due to ingress of chloride ions to the steel surface or carbonation of concrete cover. The pH of concrete pore solution is normally above 12. In such an alkaline environment, an oxide film is formed on steel surface, which protects steel from corroding. It is referred to as steel passivation. Both carbonation and chloride ingress cause this oxide film to breakdown [29, 49] steel is then depassivated and corrosion process is initiated. The corrosion of steel in concrete is essentially an electrochemical process involving two half-cell reactions occurring simultaneously at steel surface (Figure 1.4). The anodic reaction is the oxidation of iron in aqueous environment, represented by the following half-cell reaction [21, 29].



To preserve electro-neutrality, electrons produced by this anodic reaction are consumed by oxygen reduction reaction at cathodic sites on the steel surface [29, 33].



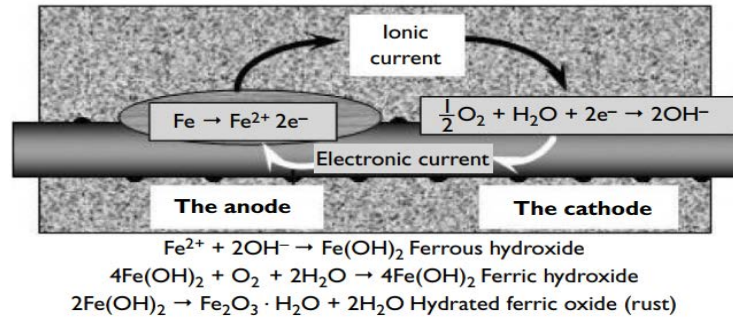


Figure 1.4: The cathodic, anodic, oxidation and hydration reaction for corroding steel [48].

When Fe^{2+} ions react with hydroxide ion OH^- and produce ferrous hydroxide $\text{Fe}(\text{OH})_2$, which forms on the surface of the reinforced steel. At the outer surface of this oxide layer, oxygen reacts with the ferrous hydroxide to form hydrous ferric oxide or ferric hydroxide, and then becomes hydrated ferric oxide. The majority of ordinary rust consists of hydrous ferric oxide and is orange to red-brown in color [21,49]. Unhydrated ferric oxide Fe_2O_3 has a volume of about twice that of the steel it replaced when fully dense. When it becomes hydrated it swells even more and becomes porous. The volume is increased two to ten times at the steel-concrete interface. This leads to the cracking and spalling that we observe as the usual consequence of corrosion of steel in concrete, rust in the bar and the rust stains could be seen easily at cracks in the concrete [48].

1.5 ELECTROCHEMICAL TECHNIQUES USED FOR CORROSION DETERMINATION

1.5.1 Half-Cell Potential Technique

The half-cell potential method is the most broadly utilized procedure of corrosion measurement of the steel rebars in concrete. This method depends on estimating the electrochemical capability of the steel rebar concerning

a standard reference electrode placed on the surface of the concrete and can provide an indication of the corrosion risk of the steel. A sponge is used to improve contact between the reference electrode and the surface of the concrete. The suggested reference electrode by ASTM is a copper/copper sulfate electrode. It should be noted that the probability of corrosion and not the actual corrosion rate could be determined by this technique.

1.5.2 Linear Polarization Resistance

In the LPR technique, a consistent potential signal are connected for a specific period of timeframe, which is determined by the time for the current to reach steady state in the form of a square wave between the working electrode steel bar in concrete and the reference electrode; and the response current I is measured. By using R_p and Stern–Geary equation, corrosion current can be computed.

1.5.3 Electrochemical Impedance Spectroscopy

The EIS technique for reinforced concrete has expanded astoundingly as of late. Investigation of the system response can provide information about the double-layer capacitance interface, structure, reactions that are taking place, corrosion rate, and electrolyte environment resistance. EIS studies the system response the impedance of a system to the application of a small amplitude alternating potential usually 20 mV signal at different frequencies.

1.5.4 Potentiodynamic Cyclic Polarization

The cyclic Potentiodynamic polarization method is a moderately non-destructive estimation that can give data about the corrosion rate, corrosion potential, and susceptibility to pitting corrosion of the metal. The procedure is built on the idea that predictions of the behavior of a metal in an environment can be made by forcing the material from its steady state condition and monitoring how it responds to the force as the force is removed at a consistent rate and the system is reversed to its steady state condition.

1.5.5 Galvano-dynamic Polarization

Galvano-dynamic polarization alludes to a procedure in which current that is continuously changed at a selected rate is applied to an electrode rebar in an electrolyte concrete pore solution. The Galvano-dynamic method plots the variation in potential versus the controlled current .This is a relatively fast method to obtain the value of R_p , and consequently, the corrosion rate.

1.5.6 Gravimetry

This is considered as the most accurate electrochemical corrosion estimation technique, all beams were autopsied. Each segment is weighed, and the measure of mass loss is determined. To perform the test, the corrosion products were removed using the Clark solution 1000 ml HCl with specific gravity=1.19 + 20 g antimony trioxide Sb_2O_3 + 50 g stannous chloride $SnCl_2$, according to the ASTM G1-90 standard procedure. This solution is effective in cleaning corrosion products at room temperature. The steel segments were immersed in Clark solution

until the corrosion products were entirely removed. The time depends on the extent of the corroded area and could be more or less than 30 min. Due to the toxic nature of the Clark solution, the cleaning procedure must be carried out under a fume hood with safety glasses and gloves. Using the area under the corrosion current density versus time curves, the cumulative mass loss was calculated and compared to the actual mass loss obtained by the Gravimetric technique.

1.6 ACCELERATED CORROSION TESTING

Normally concrete provides a good resistance to corrosion due to its another important characteristic i.e. the high alkalinity of the pore solution, which is comprised of mainly sodium and potassium hydroxides, with a pH ranging from 12.6 to 13.8. At this pH level, a protective (or passive) film is spontaneously formed during the early stages of cement hydration. This passive film may grow to a thickness of the order of 10^{-3} to $10^{-1} \mu m$ and contains hydrated iron oxides [30]. The theory of the existence of this passive layer is based on indirect evidence of anodic polarization measurement. There is still much to be learned concerning this passive film, such as the conditions of its formation, and its chemical and mineralogical composition. It is possible that this passivation film consists of several phases [22]. The concrete cover also provides good physical protection to steel from chloride ions and prevents carbonation. Therefore, it takes a long time for steel to depassivate and allow corrosion process to start. That makes it very difficult to replicate, study and to understand the corrosion phenomena in laboratories. To overcome this problem Accelerated Corrosion Tests were developed, by using them we can induce corrosion in reinforced concrete samples in laboratory in short period of time [23, 32].

Tuutti [36] proposed a corrosion model according to which the corrosion process can be divided in two distinct time phases: initiation phase and propagation phase (Figure 1.5). The initiation phase corresponds to the progressive ingress of the aggressive agents like carbon dioxide CO_2 and chloride ions Cl^- through the concrete cover. As we know now, concrete provides excellent protection for steel reinforcement thanks to the high alkalinity of concrete pore solution. The quality of the concrete cover is also involved in the physical protection of steel from environment, because concrete transport properties control the ingress kinetics of aggressive

agents. During this phase, no corrosion occurs and it usually takes many years for aggressive agents to reach steel surface and depassivate steel [23].

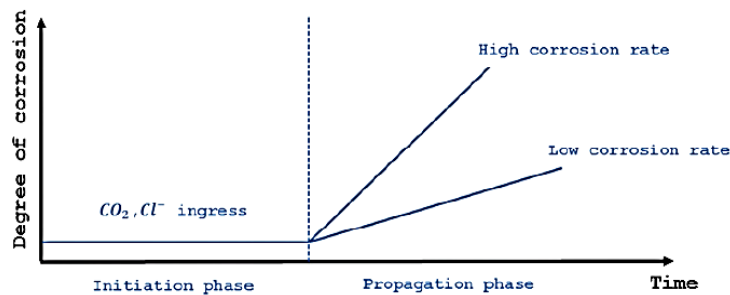


Figure 1.5: Corrosion model [36]

The laboratory acceleration of corrosion is primarily consists on the acceleration of the initiation phase so that the depassivation of steel is quickly achieved.

1.6.1 Artificial Climate Technique

In this technique corrosion, process is accelerated by way of high temperature, high humidity, and repeated wetting-and drying cycles. Artificial environment techniques, in which the samples are kept in controlled environment, are often used to accelerate initiation period. The artificial climate conditions given by Dimitri [19] that temperature = 40°C (104 ° F), relative humidity (RH)= 80%, and salt water (5% NaCl solution) spraying (1 hour) and infrared light shining (7 hours) for the wetting-and-drying cycle. The most commonly used techniques are:

- Carbonation chamber with 50% CO₂ and 65% RH,
- Samples contaminated by 3-5% NaCl solution (permanent immersion or wetting-drying cycles).

The corrosion process and corrosion characteristics of the steel bar under artificial environments are similar to that of corrosion under natural environment. Artificial climate environment as an accelerated laboratory test method is more representative than the galvanostatic method.

1.6.2 Impressed current technique/ Galvanostatic method

The impressed current technique consists of applying a constant current from a DC source to the steel embedded in concrete. After applying the current for a given duration, the degree of induced corrosion can be determined theoretically using Faraday's law, or the percentage of actual amount of steel lost in corrosion is calculated with the help of a gravimetric test conducted

on the extracted bars after subjecting them to accelerated corrosion. Using the actual amount of steel lost in corrosion, an equivalent corrosion current density can be determined. At first to de-passivate the steel, the samples were immersed in a solution of 3-5% NaCl for specific time depending on concrete quality (few weeks to a year) [32]. Then direct electric current is impressed on the steel according to the setup shown in Figure 1.6. The steel bars (main tensile reinforcement in the beam) act as the anode and the stainless bar in the center of the beam section acts as the cathode in the setup, as shown in Figure 1.6.

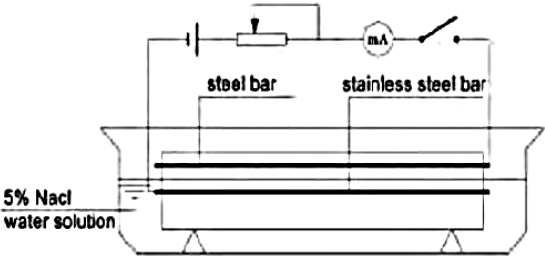


Figure 1.6: Schematic of Galvanostatic technique to induce corrosion [23]

Many researchers have used these techniques to induce the corrosion in reinforced concrete, and studied the concrete behavior after corrosion, e.g. Ormellese [26], performed accelerated corrosion test on concrete prism samples, the acceleration of corrosion was achieved by applying a direct current on the steel reinforcing bars by means of external power supplies. One of these power supplies allow application of a constant current and have a current accuracy of 61% at 500 mA full scale. The circuit was assembled in series for each group, as shown in Figure 1.7. The direction of the current was adjusted so that the reinforcing steel served as the anode, while the stainless steel bar served as the cathode, so those electrons would flow from anode to cathode.

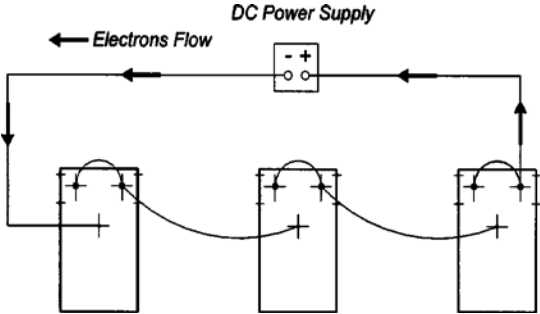


Figure 1.7: Accelerated corrosion test setup [30]

Ahn [31] have used impressed current technique to induce the corrosion to study the durability of marine concrete structure. Galvanostatic technique was also used to accelerate reinforcement corrosion by impressing anodic direct current. The beams samples were connected in series with the constant current flowing through all the beams Figure 1.8. Stainless steel bars were used as the counter electrodes; working electrode and counter electrode bars were mounted in parallel near the concrete surfaces in the maximum bending moment region Current levels applied during the wet cycle were changed to observe the change of behavior of the beams at different current levels.

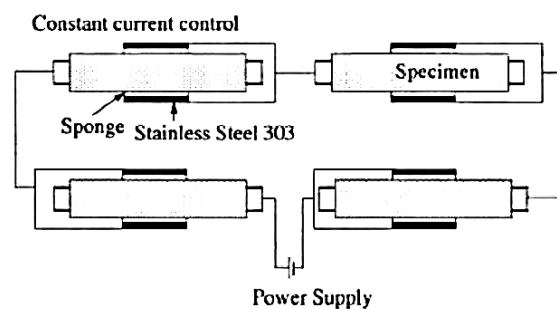


Figure 1.8: Arrangement of Accelerated corrosion test [32].

Ahmad [21] have also performed accelerated corrosion test. The set-ups used for inducing reinforcement corrosion through impressed current consist of a DC power source, a counter electrode, and an electrolyte. The positive terminal of the DC power source is connected to the steel bars (anode) and the negative terminal is connected to the counter electrode (cathode). The current is impressed from counter electrode to the rebars through concrete with the help of the electrolyte normally sodium chloride solution.

CHAPTER 2

LITERATURE REVIEW

2.1 GENERAL

This chapter deals with brief review of literature about the influence of corrosion on reinforcement. The corrosion was induced mainly by accelerated current method and further effects were studied. Literature regarding various techniques for measuring corrosion were also discussed. This chapter discusses the past research conducted by various researchers to study the different methodology used in understanding of tests setup and results. This chapter gives a complete review of the findings along with directions for future explorations.

2.2 EFFECTIVENESS OF IMPRESSED CURRENT TECHNIQUE TO STIMULATE CORROSION OF STEEL REINFORCEMENT IN CONCRETE BY A. TAMERET AL[29]

In this paper, the main objective of the study were to examine the effect of varying impressed current density levels on the strain behavior of concrete due to expansive stress by corrosion, crack width and pattern, and mass loss due to corrosion by a constant current supply maintained with automatic crossover. Twelve number of singly reinforced prism samples with two bars of diameter 11.3 mm were casted. The dimensions of the prism defined were 300 mm long with cross section 150 mm × 250 mm. A stainless steel bar of diameter 6mm placed at a distance of 100 mm from top in order to act as cathode and the reinforcement as anode in the corrosion generating process. Five percent NaCl by weight of cement added to concrete mix to accelerate corrosion. The specimen were grouped in four categories A, B, C and D. Impressed current density levels for each group were 100, 200, 350 and 500 μ A/cm² and the corrosion time recorded was 815, 766, 380 and 306 hours respectively. The experiment used Demountable Mechanical strain Gauge for strain measurement, which resulted that using a low density of current produced realistic corrosion, as slow dissipation of corrosion products took place at low current densities. A high concentration of corrosion products around the reinforcing bars caused more expansion and internal stresses, which lead to further degradation of the concrete around the steel reinforcing bars and width of cracks became large. All developed cracks were parallel to the reinforcement. The measured degrees of corrosion agreed with the expected ones based on

Faraday’s law at different level of current density. Therefore, impressed current is a reliable technique to simulate corrosion of steel reinforcement in concrete.

2.3 EFFECTS OF RUST AND SCALE OF REINFORCING BARS ON THE BOND PERFORMANCE OF REINFORCEMENT CONCRETE BY C. H. HUANG[10]

In this study, accelerated corrosion method processed corrosion in the reinforcement for investigating the bond properties between reinforcement and concrete. Two deformed bars of diameter 9.5mm and 19mm were casted in a cube of side 150mm separately to perform a pull out test. Two heads divided the experiment: first being 100% corrosion on whole surface and the other was partial-surface corrosion of 40, 60 and 100%. The two groups were prepared for four levels of corrosion (3, 5, 10, and 15%). The degree of corrosion measured is the loss in weight of the steel bar relative to the weight of unit length before corroding. To calculate the corrosion depth, the following equation is used:

$$d = s \times d_b / 4 \text{----- Eq. 2.1}$$

Where, d = the corrosion depth (mm); s = Weight loss of bar/Original weight of bar; d_b = diameter of steel bar. The greater the diameter of steel bar the longer the duration for producing corrosion and more the depth rate of corrosion. The tensile strength of steel decreases with an increase in corrosion level. There was no significant change in the yield and ultimate strength for partial surface corrosion. The bond strength increased when the corrosion was less than 3% [20] but an increase above this value decreased the bond strength (Figure 2.1).

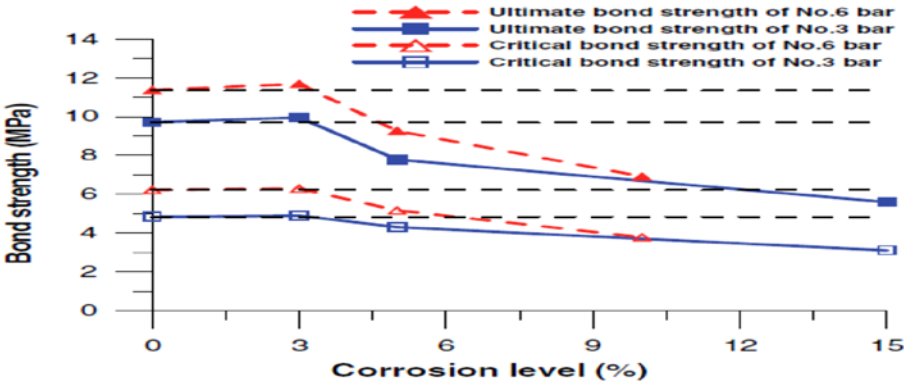


Figure 2.1: Effect of corrosion level on the bond strength of steel bars[10]

2.4 ADVANCED METHODS OF CORROSION MONITORING - A REVIEW BY N.G. RATHOD, N.C. MOHARANA [9]

The main cause of degradation of steel reinforcement in concrete is corrosion. Corrosion begins earlier in the reinforcement before the appearance of cracks. Some non-destructive methods to detect corrosion were discussed in this study, as it is not possible to detect corrosion by visual means. In this paper, various non-destructive methods to monitor corrosion using different equipment were defined.

Open circuit potential technique (OCP) worked on the principle of measuring corrosion potential of rebar in comparison with standard reference electrode mostly saturated calomel electrode (SCE). In Surface Potential (SP) technique, an electric current flowed between anodic and cathodic sites in the concrete during corrosion and sensed by measuring the potential drop in concrete. Linear Polarization Resistance (LPR) technique only needed a connection to the steel reinforcement to measure corrosion of reinforced steel in RC structures. Potentiodynamic Anodic Polarization classifies a metal sample by its current-potential connection. These above-mentioned techniques proved useful in only finding the anode and cathode position and failed to provide real time corrosion result. Whereas for measuring real time corrosion methods like AE, Galvanic Monitoring Probe, FO, High Frequency UV overcome the limitation.

2.5 LABORATORY SIMULATION OF CORROSION DAMAGE IN REINFORCED CONCRETE BY F. U. A. SHAIKH ET AL [6]

This study presents an experimental program to compare corrosion damage using two accelerated corrosion techniques namely, constant voltage and constant current. In this study, six concrete columns were tested. Total of six reinforced deformed bars of diameter 13mm and spiral of 6mm diameter were placed longitudinally. A stainless steel pipe of diameter 20mm placed in the center of the column to act as cathode. To speed up corrosion and to supply oxygen small holes of diameter 2mm and four in number were made along the steel pipe longitudinally. The study consisted of two parts. The first part allowed corrosion around 8 % steel loss using two methods, constant voltage and constant current. The second part was to corroded the columns up to failure by maximum compression load. In the constant current sampled column, longitudinal cracks, crack width and circumferential expansion were more prominent than in constant voltage. Conclusions draws that almost similar steel loss took place but more damage was caused by constant current. As a result great structural damage by constant current as the

load carrying capacity also decreased. Therefore, the constant current method gave more desired results to stimulate corrosion in reinforced concrete member.

2.6 EXPERIMENTAL AND NUMERICAL INVESTIGATION OF CORROSION-INDUCED COVER CRACKING IN REINFORCED CONCRETE STRUCTURES BY M. G. STEWART ET AL[19]

In this paper investigations based on experiments and numerical calculations checked the initiation and propagation of cracks by induced corrosion considering the concrete cover (25,50mm) and water cement ratio (0.45,0.5,0.58). For experimental setup, an accelerated corrosion method was set up to induce corrosion in eight rectangular slab specimen (700 mm×1000 mm×250 mm). Accelerated corrosion rate of $100\mu\text{A}/\text{cm}^2$ passed through the reinforcement to get corrosion in desired time. A linear potentiometer displacement transducers (POTs) joined on both sides to observe crack propagation. The rust developed during the process of corrosion of reinforcing steel in concrete breaches into the concrete pores and micro cracks are developed [18]. A finite element modelling in ABAQUS was done. The model-evaluated amount of corrosion products penetrated in concrete pores and cracks and therefore, did not contribute to crack initiation and propagation. In this study, the amount of corrosion products penetrating in the concrete pores before crack initiation is larger than that obtained by other experiments.

2.7 ESTIMATING CRITICAL CORROSION FOR INITIATION OF LONGITUDINAL CRACKS IN RC STRUCTURES CONSIDERING PHASES AND COMPOSITION OF CORROSION PRODUCTS BY SUDHIR MISRA ET AL [7]

In this study, a critical corrosion at the onset of crack formation considered the production of rust at steel concrete junction was observed. The various expansive products of corrosion exert radial pressure on the cover of concrete that lead to the formation of longitudinal cracks. Further the product of corrosion by accelerated corrosion method were determined using spectroscopic and microscopic method and then compared to natural corrosion of reinforcement in an old building nearly 50 years old. A combination of phase wise mass loss calculations and along with corrosion pressure theory estimated the critical corrosion amount. Various rust phases developed such as goethite, lepidocrocite, akageneite, maghemite, and magnetite. Spectroscopic

studies showed some similarity in the rust phases formed under natural corrosion and those formed during accelerated corrosion.

This study also concluded that, as the cover-to diameter ratio increased, the critical corrosion amount increased. A radial pressure increased with the loss in weight of the reinforcement at the commencement of corrosion. Further, as the concrete strength increased, critical mass loss and its associated critical corrosion pressure also increased.

2.8 EVALUATION OF THE MECHANICAL PROPERTIES OF STEEL REINFORCEMENT EMBEDDED IN CONCRETE SPECIMEN AS A FUNCTION OF THE DEGREE OF REINFORCEMENT CORROSION BY H.S. LEE AND Y.S. CHO [20]

In this experiment, the tensile strength test conducted at various stages of corroded reinforcement concluded that the chloride-induced corrosion produced pitting effect and the usage of electrical current lead to uniformed corrosion. With increase in degree of corrosion, the nominal yield point and nominal elastic modulus decreased. The mechanical properties of reinforcement corroded by chloride-induced damage were less than that of reinforcement corroded by electric method, even when the rate of mass loss by corrosion are the same. The rate of reduction of yield point proved to be greater than rate of reduction of elastic modulus at same corrosion percentage due to occurring local stresses.

2.9 A MODEL FOR PREDICTING TIME TO CORROSION-INDUCED COVER CRACKING IN REINFORCED CONCRETE STRUCTURES BY C.H. LU ET AL [18]

This paper presents a mathematical model that predicted time of corrosion initiation and cover cracking time. Some basic assumptions considered in the study were as follow:

- (i) Corrosion process was uniform around the steel reinforcement which resulted in a uniform radial expansive pressure at the steel-concrete interface,
- (ii) The concrete around the steel reinforcing bar was modeled as a thick-walled cylinder and the wall thickness equals to the thinnest concrete cover,
- (iii) The stresses in concrete and reinforcement were induced only by the expansion of corrosion products, and
- (iv) The radial cracks will develop from the cylinder's inner surface to outside,

Further, Faraday's law helped to predict the time from corrosion initiation to cover cracking. It was seen that time for cover cracking could be prolonged by increasing the cover thickness (Figure 2.2), decreasing the bar diameter (Figure 2.3), enhancing the concrete strength (Figure 2.4) and controlling the level of oxidation (Figure 2.5) can lead to good structural durability. The author verified the result with previously proposed works and proved to give a reasonable prediction for cover cracking and analysis for service life of the structure.

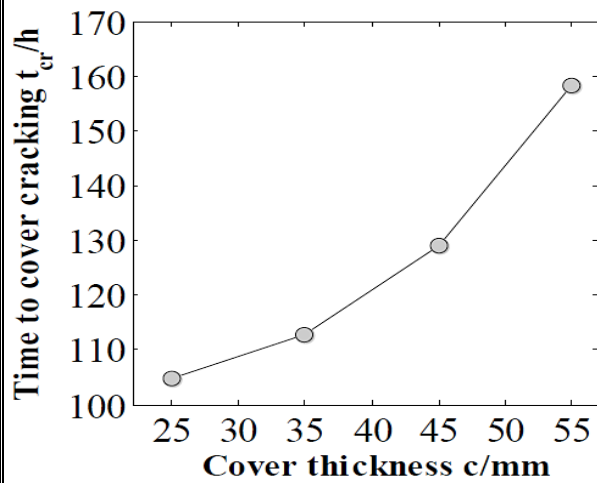


Figure 2.2: Relationship between time to cover cracking and cover thickness [18]

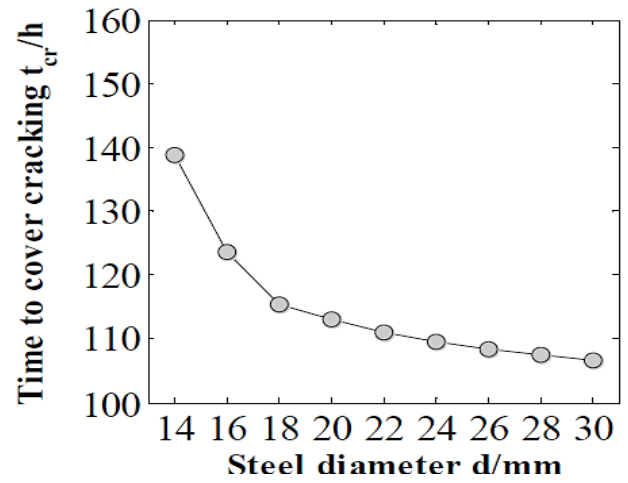


Figure 2.3: Relationship between time to cover cracking and steel diameter [18]

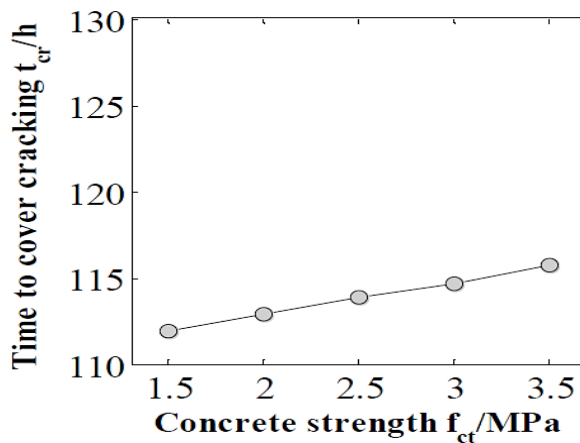


Figure 2.4: Relationship between time to cover cracking and tensile strength of concrete [18]

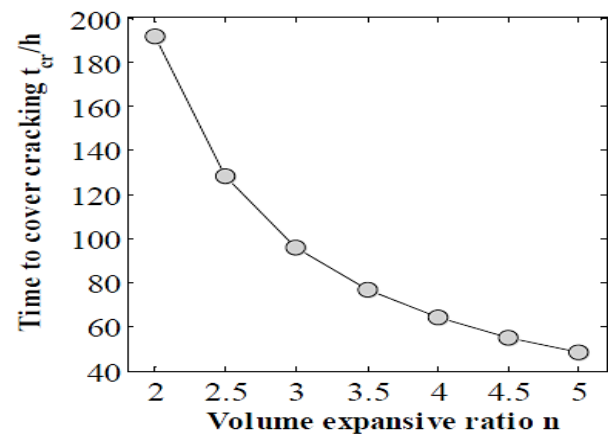


Figure 2.5: Relationship between time to cover cracking and volume expansive ratio [18]

2.10 MODELING CORROSION-INDUCED CRACKING IN REINFORCED CONCRETE BY S. HUO [8]

This study developed a model that predicted time from corrosion initial to corrosion cracking. No internal force action on steel- concrete interface was considered before the corrosion products filled the concrete pores. A relationship between internal expansion pressure and steel mass loss was established. The model was set as a thick walled cylinder and assumed the wall thickness equal to the concrete cover and the concrete cracking when the internal expansion pressure exceed the strength of concrete. Later the results compared to the computed model accuracy with the experiment result proved to be within the permissible range. Therefore, this forecasting of corrosion induced cracking is feasible.

2.11 FACTORS CONTROLLING CRACKING OF CONCRETE AFFECTED BY REINFORCEMENT CORROSION BY C. ALONSOL ET AL [32]

This paper worked on quantifying the relation between the amount of corrosion and cover cracking. Various parameters were considered during the study namely cover to diameter ratio, proportions of cement, water cement ratio, cast position of the bar, transverse reinforcement and corrosion rate. Corrosion induced by accelerated corrosion method by making the rebar as anode. The initiation of cracking took place in two steps, generation and propagation. Two specimens were casted: specimen 1 with dimensions $15 \times 15 \times 38$ cm and the bars used were of diameter 3, 8, 10, 12 and 16mm. The cover used was 10,15,20,30,50 and 70mm. The reinforcement were placed in center and corner (Figure 2.6). Specimen 2 with dimensions $30 \times 30 \times 30$ cm with and without the transverse reinforcement and the diameter of reinforcement was 16 mm and that of rebar was 6 or 8 mm (Figure 2.7).

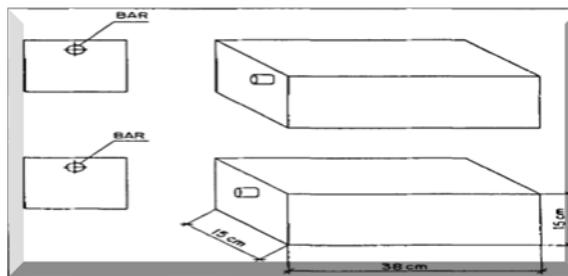


Figure 2.6. Specimen 1 [32]

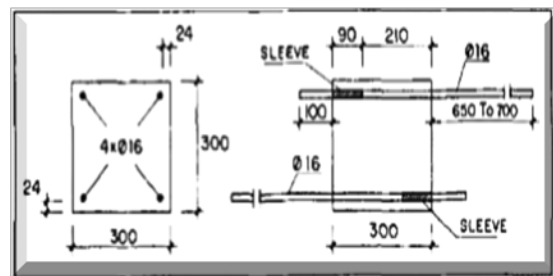


Figure 2.7. Specimen 2 [32]

2.12 ANALYSIS ON COMPRESSIVE STRENGTH OF CONCRETE WITH PARTIAL REPLACEMENT OF CEMENT WITH ALCCOFINE BY P.R.K CHAKRAVARTHY AND R.R. RAJ [1]

In this paper presence of Alccofine in the ordinary cement in ideal measurements can be relied upon to enhance the compressive strength and give protection against chloride assault, ocean water assault and quickened erosion assault. The primary target of the work centers on the compressive quality of cement with incomplete replacing of concrete with Alccofine. Replacement of cement in M25 mix with alccofine in varying percentage at 0%, 4%, 8%, 16%, 17%, 20%, 25%, 50%, 75% and 100% for 7 and 28 days the compressive strength was maximum at 16% replacement exhibiting the value of 50.95 % and 60.95%, and on further increase the value decreased as shown in the Figure 2.8 and Figure 2.9.

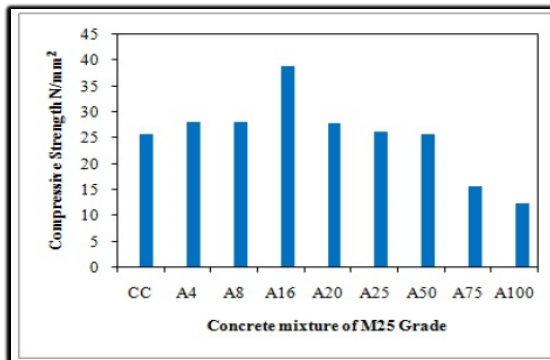


Figure 2.8: Compressive strength of concrete with various percentage of alccofine for 7 days curing [1]

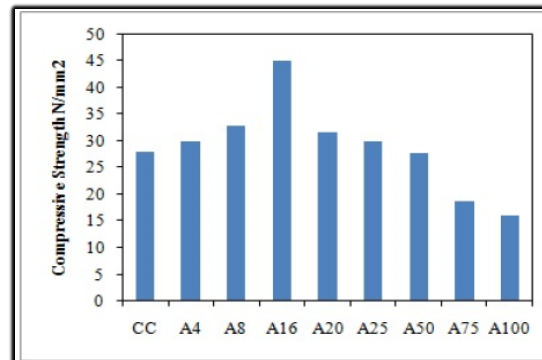


Figure 2.9: Compressive strength of concrete with various percentage of alccofine for 28 days curing [1]

Alccofine when added in concrete mix displays decent permeability parameters that brings about resistance against corrosion. CaO present in alccofine when consolidates with water under mix, gives high resistance against chemical and acid attacks.

2.13 A STUDY ON CORROSION OF REINFORCEMENT IN CONCRETE AND EFFECT OF INHIBITOR ON SERVICE LIFE OF RCC V. KUMAR ET AL [11]

The author did extensive research to develop models that predicts the time for corrosion initiation. The study reveals that though Calcium palmitate and its combination with calcium nitrite decrease the concrete strength but inhibition to the corrosion of the rebar increases the service life of the Reinforced concrete by 8 to 10 times. Various factors affected corrosion like:

1. Effect of carbonation and entry of gaseous pollutants

2. Effect of aggressive anions
3. Effect of Bacterial action
4. Effect of w/c ratio
5. Effect of cover over reinforcing steel

Corrosion procedure of Reinforcement in concrete begins with depassivation i.e. loss of oxide layer over the rebar and after that, it reaches a basic stage at which corrosion would create spalling of concrete cover or breaking through the entire concrete as portrayed in Figure 2.10. The stages of rebar corrosion depicts the service life prediction of the structure.

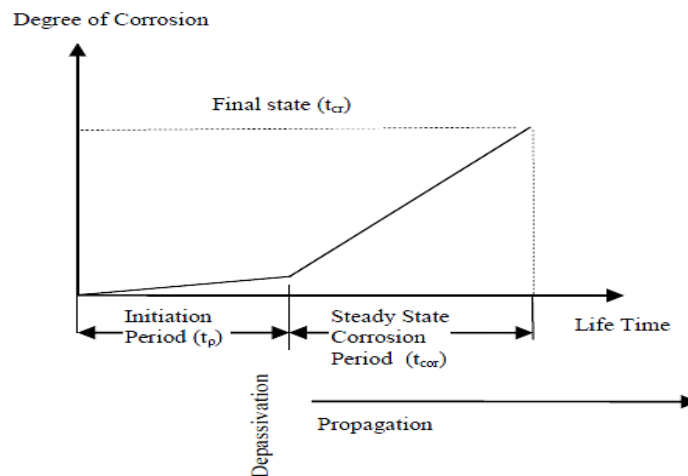


Figure 2.10: The stages of rebar corrosion [11]

2.14 STEEL FIBER REINFORCED CONCRETE BY N.V. CHANH [52]

In this report, the author describes the importance of steel fiber reinforced concrete in crack resistance and propagation. As a result of the ability to arrest cracks, fiber composites possess increased extensibility and tensile strength, both at first crack and at ultimate, particular under flexural loading; and the fibers are able to hold the matrix together even after extensive cracking. The paper discussed the mechanic properties, technologies, and applications of SFRC. Fibers do little to upgrade the static compressive strength of concrete, with increments in strength extending from basic nil to maybe 25%. Indeed, even in individuals that contain ordinary reinforcement notwithstanding the steel fibers, the fibers have little impact on compressive strength. In any case, the fibers do generously expand the post-splitting pliability or energy assimilation of the material, Fibers adjusted toward the ductile pressure may achieve extensive increments in direct tensile strength, as high as 133% for 5% of smooth, straight steel fibers. In

any case, for haphazardly disseminated fibers, the expansion in strength is considerably small, running from as meager as no increase in a few cases to 60% in others.

2.15 RESEARCH GAP

After studying literature papers, some research gaps were found:

- There is a void in literatures which do not provide information about uses of mineral admixtures and fiber additives together in prevention of corrosion.
- Limited literatures are available on the effect of corrosion of concrete with mineral additives.
- Degree of induced corrosion quantification is also limited.

2.16 RESEARCH OBJECTIVES

- To study the effect of corrosion by variation of steel diameter on concrete beam.
- To study the effect of corrosion in steel fiber reinforced concrete incorporating ultrafine slag.
- Comparative study of the above two objectives.

CHAPTER 3

EXPERIMENTAL INVESTIGATIONS

3.1 GENERAL

In these chapter different material properties and detailed experimental program and procedure has been discussed. Tests on cement, fine aggregate and coarse aggregate were performed. Normal consistency, initial and final setting time, compressive strength and tensile strength test have been performed on cement. Specific gravity and grading of fine aggregates. Whereas water absorption and specific gravity on coarse aggregate were done according to their respective Indian Standards code. Various factors which directly or indirectly effects the properties of concrete is discussed so that the experimental program can be designed to investigate the induced levels of corrosion on different reinforce concrete samples.

3.2 MATERIALS USED

Concrete is a hard material that includes cementitious medium inside which aggregates are implanted. Potential quality and strength of concrete of a given mix proportion are particularly subject to the level of its compaction. The materials utilized for planning of concrete are inspected in the accompanying sections.

3.2.1 Aggregates

Aggregates are the basic constituents in concrete. They offer body to the concrete and help in decreasing shrinkage. Aggregates give great effect on quality, durability and dimensional steadfastness to concrete [51]. No under 75% of the volume of concrete is controlled by aggregates. The aggregates are portrayed in view of their weight and size. The quality of concrete, can't outperform the quality of the aggregates that constitute it. In any case, it isn't possible to explicitly test total for its quality. An ordinary estimation of the staggering strength of aggregate for concrete is appropriate from 80-100MPa. The firmness of total is basic for keeping up the dimensional reliability of concrete under load. However aggregates of direct quality and modulus of flexibility can positively be used to withstand the volume changes of concrete coming to fruition due to thermal or expansive causes. Aggregates are angular or round to fit as a fiddle. The surface of aggregates characterizes the smoothness. The tough texture of

aggregate will provide a better cement-aggregate bond and hence it is preferred. On the basis of weight aggregates are classified as:

- a) Normal weight aggregate
- b) Light weight aggregate
- c) Heavy weight aggregate

Normal weight aggregate is further classified as natural aggregate and artificial aggregate. Example sand is natural aggregate and broken brick, air-cooled slag etc. are artificial aggregate.

Aggregates can also be further classify based on their size

- a) Coarse aggregate ($> 4.75\text{mm}$)
- b) Fine aggregate ($< 4.75\text{mm}$)

Aggregates assume a critical part to create high quality concrete. In this investigation total utilized is coarse total having an extreme size of 20mm. This utilization depends on the past research, which demonstrated that the utilization of little coarse aggregate prompts increment in concrete quality in contrast to bigger size aggregate.

All the regular aggregates begin from bedrock. There are three sorts of rocks in particular, igneous, sedimentary and metamorphic. Out of these three igneous rocks, make exceedingly attractive concrete since they are hard, dense and tough. The dimension of the aggregate is likewise an essential trademark since it influences the workability of concrete. From outlook perspective of the economy in cement prerequisite for a given water-cement proportion round aggregate are desirable over angular aggregate [51]. Surface measures the relative degree to which molecule surfaces are cleaned or dull, smooth or harsh. As the surface smoothness builds contact region diminishes, subsequently, a profoundly cleaned particle will have a less holding territory with the matrix than a rough particle of a similar volume. The degree of coarse aggregates assumes an imperative part of workability and concrete finishes. The degree of fine aggregate influences the workability and completing of concrete. Grading is a vital property of aggregate utilized for making concrete, in perspective of the packing of particles, causing the lessening of voids. This in turns affects the water requirement and cement content of concrete. Courses of action of IS sieves for analysis appears in Figure 3.1. Evaluating is portrayed in terms of cumulative percentage of weights passing a particular IS sieve [40, 41]. The grading limits for coarse and fine aggregate are explained in IS 383-1970 [40]. Fineness modulus is a gross measure of aggregate gradation and is associated with fine aggregates. This is incorporated in

the mix proportioning process. It is defined as the sum of the cumulative percentage of weight retained on a standard set of sieves divided by 100. Classification of fine aggregates based on fineness modulus is tabulated in Table. 3.1.

Table 3.1 Classification of fine aggregates based on FM [49]

Type	Fineness modulus (FM)
Fine	2.3-2.6
Medium	2.6-2.9
Coarse	2.9-3.2



Fig. 3.1: IS sieves for sieve analysis.

3.2.2 Binder

3.2.2.1 Portland Pozzolana cement

The main raw material for production of cement is clinker. Clinker is an artificial rock made by heating limestone and other raw materials in specific quantities to a very high temperature in a specially made kiln. Portland cement is hydraulic cement made by finely pulverizing the clinker produced by calcining to development of fusing a mixture of argillaceous and calcareous materials. It is the fine grey powder that is the most important ingredient of concrete as it undergoes a chemical reaction. Portland Pozzolana cement (PPC) is manufactured by the mixing

the OPC clinker with 10 to 25 per cent of pozzolanic material (as per the latest amendment, it is 15 to 35%). A pozzolanic material is essentially a siliceous or aluminous material which itself possesses no cementitious properties, and in the presence of water, reacts with calcium hydroxide, liberated in the hydration process at ordinary temperature, to form compounds possessing cementitious properties. The pozzolanic materials generally used for manufacture of PPC are calcined clay or fly ash. Fly ash is a waste material, generated in the thermal power station, when powdered coal is used as a fuel. These are collected in the electrostatic precipitator [49].



Fig. 3.2: Pozzolana Portland cement

3.2.2.2 Alccofine

Ultra-fine slag or Alccofine is a further developed type of GGBS in which slag is further ground to under 20 microns. Therefore, its specific surface area is expanded significantly to 3000-5000 m²/kg (Bet Analysis). Molecule state of ultrafine slag is spherical (Scanning electron magnifying lens) which gives expanded workability at much diminished water content due to ball bearing action. Pozzolanic reaction rises because of increment in the specific surface area. Silica content is observed to be over 80%, therefore, it behaves as a decent pozzolanic material. Segregation and bleeding are not seen subsequently, giving a decent impermeable material which in turns expands its durability. A joint venture with Ambuja cement ltd and Alcon engineers produces ultrafine slag with a brand name Alccofine. It is made in the controlled conditions with exceptional gear to create optimized particle distribution which is its extraordinary property (Table. 3.2). Alccofine 1203 (Figure 3.3) and Alccofine 1101 are two sorts of Alccofine with low calcium silicate and high calcium silicate respectively. Alccofine 1200 has a series of 1201, 1202, 1203 which speaks to fine, micro fine, ultrafine particles size

respectively. Alccofine 1203 is slag based SCM having ultra fineness with enhanced particles size distribution and Alccofine 1101 is a micro-fine cementitious grouting material for soil adjustment and rock stabilizing. The execution of Alccofine is better than the various admixtures utilized as a part of India.



Figure 3.3: Ultra-fine slag

Table 3.2: Physical and chemical properties of alccofine

Fineness	Specific gravity	Bulk density	Particle size		
			D10	D50	D90
>12000cm ² /kg	2.9	700-900kg/m ³	1.5μ	5μ	9μ
Chemical Properties					
CaO	SO ₃	SiO ₂	Al ₂ O ₃	Fe ₂ O ₃	MgO
61-64%	2-2.4%	21-23%	5-5.6%	3.8-4.4%	0.8-1.4%

3.2.3 Steel Fiber

Steel fiber was added to reinforced concrete to affect various parameters. The actual role of the fibers is to reduce the corrosion in the reinforcement. During the progress of impressed current the concrete acted as a medium for transportation of ions so the steel fiber would be affected first. One could suspect that the steel fiber would act as a sacrificing material in order to protect the reinforcement. . An increase in the rate of corrosion will give a rapid break down of thin fibers. Crimped steel fibers were used for this study. The tensile strength and the Young's modulus of the used steel fibers were 1250 MPa. Other properties of the used steel fibers are summarized in Table 3.3.

Table 3.3: Properties of used steel fiber.


Length	50mm	
Diameter	1mm	
Appearance	Clear and Bright	
Tensile strength	800-2500 MPa	
Shape	Undulated along its length	
Size	0.8mmx0.35mm	
Aspect ratio	43.75	

Figure 3.4:Steel fibers

3.2.4 Water

One cannot imagine concrete without water. Water is the following most ingredient after cement for making concrete. Reckless utilization of water can prompt low quality concrete. In this way a proper quality and quantity investigation of the amount of water required for making great quality concrete is fundamental. The water utilized can be either to mix concrete or for curing. At the point when water is included then, hydration reaction begins which form strength giving C-S-H gel. It is all around accepted that if water is appropriate for drinking than it is reasonable for making concrete. Water appropriate for making concrete is additionally decided by its pH level. On the off chance, that pH level lies between 6 to 8 and free from organic mixes than it is appropriate for making concrete. The quality of concrete likewise relies upon the water-cement proportion. Figure 3.4 demonstrates a schematic portrayal of cement gel hydration with w/c proportion 0.2, 0.3 and 0.5. It can be noticed that a little measure of water is expected to hydrate cement. Extra water is required to grease up the blend. An excessive amount of water can lead to the creation of capillary pores. Excess of water adds to the workability of concrete, however, lessens its quality to some degree [50]. The measure of water expected to accomplish the coveted workability is typically more than that required for complete hydration of the cement.

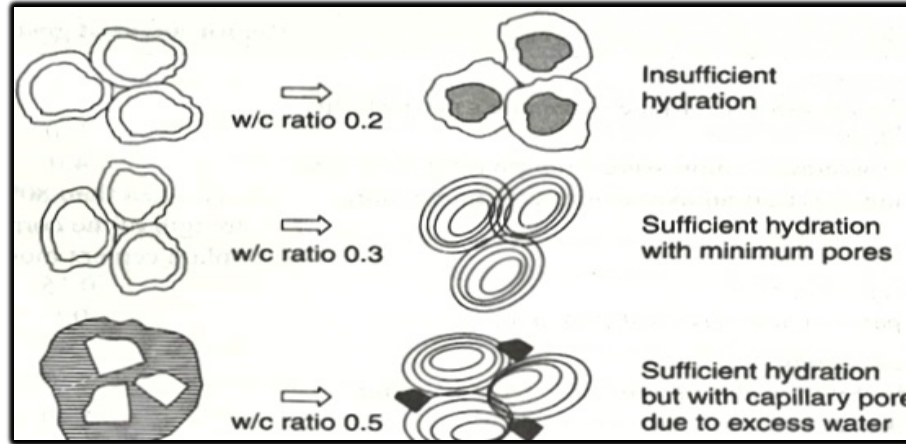


Figure 3.5: Schematic representation of insufficient, sufficient and excess water for hydration [50]

3.3 TESTING OF MATERIALS

3.3.1 Cement

3.3.1.1 Standard Consistency

The Consistency of cement test performed to determine the amount of water percentage by weight of cement added in cement to attain Standard consistency or normal consistency of cement. It is the amount of water which when added to cement attains a penetration of 5-7 mm from the bottom of the Vicat mould or 33-35mm from top of the Vicat Mould. The water requirement for various tests of cement depends on the normal consistency of the cement, which itself depends upon the compound composition and fineness of the cement. Vicat's apparatus as per IS: 4031 Part 4: 1988 [42] was used.

The Standard Consistency of cement came out to be 33%.



Figure 3.6: Standard Consistency

3.3.1.2 Initial setting time

The time at which cement starts hardens and completely loses its plasticity is called Initial setting time of cement. Within this time, cement can be moulded in any desired shape without losing its strength. It is that time period between the time when water is added to cement and the time at which 1 mm square cross section needle fails to penetrate the cement paste, placed in the Vicat's mould 5 mm to 7 mm from the bottom of the mould [43]. It is important to know the initial setting time, because of loss of useful properties of cement, if the cement mortar or concrete is placed in moulds after this time.

Initial setting time came out to be 40 minutes.

3.3.1.3 Final setting time

The time at which cement completely loses its plasticity and became hard is a final setting time of cement. Final setting time is that time between the time when water is added to cement and the time at which 1 mm needle makes an impression on the paste in the mould but 5 mm attachment does not make any impression [43]. The importance of final setting time lies in the fact that the moulds can be removed after this time

Final setting time came out to be 7 hour and 46minutes.

3.3.1.4 Specific gravity

Specific Gravity of cement is the ratio of density of cement to density of water provided temperature remains constant. Excessive exposure of cement to moisture effects workability and strength of cement. For Nominal mix design, the specific gravity of cement should be 3.15g/cc. If the cement is exposed to extreme moisture content due to bad weather conditions, then the specific gravity of cement may go up to 3.19. If the specific gravity is 3.19, then the pores in cement are filled with the moisture content. Cement undergoes premature Hydration. Specific gravity of cement is measured by density bottle method. To calculate the specific gravity of material, we generally use water. But in cement, we use kerosene for finding specific gravity. Cement hydrates in the presence of water. Cement will not undergo any reaction or change when it is mixed with kerosene.

By doing experiment in lab specific gravity of PPC cement is 2.79.

3.3.1.5 Compressive strength

Compressive strength of cement is measured by a compressive strength test on mortar cubes. Standard sand is used for making cement mortar. Compression testing machine was used for compression testing with cube size of 70.6mm×70.6mm×70.6mm.

Compressive strength after 7 days curing – 17.1 MPa

Compressive strength after 21 days curing – 23.0 MPa

Compressive strength after 28 days curing – 42.1 MPa



Figure 3.7: Compressive test on cement

3.3.1.6 Tensile strength

Tensile Strength of Cement test was previously used to have an indirect clue of compressive strength of cement. Briquettes are required for testing tensile strength of cement. The moulds of briquettes are according to the ASTM standards. A mould consists of three briquettes. These moulds are filled with cement mortar mix with cement to sand ratio 1:3. After 3 days and 7 days of curing, briquettes are tested in briquette testing machine to determine tensile Strength of cement mortar.

Tensile strength of cement after 3 days – 2.89MPa

Tensile strength of cement after 7 days – 3.35MPa

3.3.2 Sand

3.3.2.1 Specific gravity

The specific gravity of sand was determined by Density bottle. Sand particles composed of quartz have a specific gravity ranging from 2.65 to 2.80.

Weight of empty bottle (W1) = 649.0gm

Weight of bottle and soil together (W2) = 850.3gm

Weight of bottle, soil and water together (W3) = 1550.2gm

Weight of bottle and water together (W4) = 1420.2gm

$$\text{Specific Gravity of sand} = \frac{W_2 - W_1}{(W_4 - W_1) - (W_3 - W_2)}$$

Specific gravity of sand using density bottle = 2.67

3.3.2.2 Grading of Fine Aggregates

On the basis of particle size [41] fine aggregate is graded into four zones in Table 3.4.

After sieve analysis we get our results in Table 3.5 with our sample resulting in zone IV.

Table 3.4: Grading of sand on particle basis [41].

IS Sieve	Percentage passing for			
	Grading Zone I	Grading Zone II	Grading Zone III	Grading Zone IV
10mm	100	100	100	100
4.75mm	90 – 100	90 – 100	90 – 100	95 – 100
2.36mm	60 – 95	75 – 100	85 – 100	95 – 100
1.18mm	30 – 70	55 – 90	75 – 100	90 – 100
0.60mm	15 – 34	35 – 59	60 – 79	80 – 100
0.30mm	5 – 20	8 – 30	12 – 40	15 – 50
0.15mm	0 - 10	0 - 10	0 - 10	0 – 15

Table 3.5: Sieve analysis of fine aggregates with weight of sample = 1000g, we get a zone 4 fine aggregate.

Sieve	Retained on each sieve - weight (gm)	Retained on each sieve (%)	Cumulative % retained	Passing through (weight)	Passing through (%)
40mm	nil	0	0	987	100
20mm	nil	0	0	987	100
10mm	nil	0	0	987	100
4.75mm	6	0.608	0.608	981	99.39
2.36mm	8.5	0.861	1.469	972.5	98.531
1.18mm	9.5	0.962	2.431	963	97.56
600 μ	12.7	1.286	3.717	950.3	96.28
300 μ	80.1	8.116	11.832	870.2	88.167
150 μ	775.3	78.55	90.382	94.9	9.615
Passing 150 μ	94	9.523			
Total	986.1				

3.3.3 Coarse Aggregates

3.3.3.1 Water absorption

Coarse aggregate have a tendency of absorbing water from the concrete mix. This reduction in water content, if not accounted for, can cause incomplete hydration of cement.

The water absorption of aggregates ranges from 0.1 to 2.0 %.

$$\text{Water absorption} = (A-B/B)*100$$

Weight of sample = 2000g

Weight of saturated surface dried sample (A) = 1.955 kg

Weight of oven dried sample (B) = 1.925 kg

Water absorption of aggregates = 1.523%

3.3.3.2 Specific gravity

The specific gravity of aggregates was calculated by the test results of water absorption test.

Weight of saturated aggregate suspended with basket in water (W1)= 1.75kg

Weight of basket suspended in water (W2) = 0.49kg

Weight of saturated surface dry aggregate in air (W3) = 1.955kg

Weight of oven dried aggregate = 1.925kg

Specific gravity of aggregates = 2.75

3.4 MIX DESIGN

Concrete mix proportioning is represented by the properties required in the fresh and solidified state. The properties of plastic concrete are imperative for appropriate compaction. The strength and durability of a conclusive structure are given by hardened concrete. The two are connected essentially to the water-cement proportion. Proportioning a concrete mix for a given design is hence the craft of acquiring an appropriate ratio of the different elements of suitable concrete with the required properties at the most reduced cost. An appropriately proportioned concrete mix with specific necessities of workability, strength, and durability ought to have the minimum cement content to make the mix generally economic.

Mix design can be defined as the way toward choosing suitable elements of concrete and deciding their relative proportions with the question of delivering concrete of certain minimum strength and durability as monetarily as could be allowed. The motivation behind planning as can be seen from the above definitions is two-fold. The primary objective is to accomplish the stipulated least strength and durability. The second objective is to make the concrete in the most prudent way. Cost insightful all concretes depend principally on two variables; to be specific cost of material and cost of labor. Labor cost, by means of formworks, bunching, mixing, transporting, and curing is nearly same for good concrete and bad concrete. Since the cost of cement is many times more than the cost of other ingredients, attention is mainly directed to the use of as little cement as possible consistent with strength and durability. . Therefore attention is mainly directed to the cost of materials. Since the cost of cement is many times more than the

cost of other ingredients, attention is mainly directed to the use of as little cement as possible consistent with strength and durability.

3.4.1 Design Specifications

- a) Characteristic compressive strength required = 20 N/mm²
- b) Maximum size of aggregate = 20mm angular
- c) Degree of workability = 0.90
- d) Degree of quality control = Good
- e) Type of exposure = Mild

3.4.2 Test data for materials

- a) Cement used – PPC
- b) Specific gravity of cement = 2.79
- c) Specific gravity of coarse aggregate = 2.75
- d) Specific gravity of fine aggregate = 2.67
- e) Water absorption of coarse aggregate = 1.523%
- f) Ultra fine slag = partial replacement of cement by 20%
- g) Steel fiber = 1% of the total mix

Water to cement ratio : 0.45			
Water	Cement	Fine aggregate	Coarse aggregate
172.422 kg/m ³	383.16 kg/m ³	587.03 kg/m ³	1292.82 kg/m ³

Final Mix Design- 1: 1.53: 3.3

3.5 BATCHING, MIXING AND CASTING OF SPECIMENS

Rectangular moulds of 100mm x 100mm x 500mm (Figure 3.8) were used for casting of testing samples of beams. All the specimens were prepared in accordance with Indian Standard Specifications. A total of 36 samples were casted out of which 18 were made to corrode and rest for comparison purposes. Reinforcement of varying diameter (12mm, 16mm and 20mm) of grade Fe500 was used. The experiment was classified into two sets by varying clear cover of 35mm and 45mm that were further classified into three sets varying on the mix. The first set was a simple reinforced concrete (RC), next reinforced concrete by addition of steel fiber (SF)

varying 1% by volume of concrete mix and the last one by addition of ultra-fine slag by replacement of cement (ASF) by 20% along with 1% steel fiber addition (Figure 3.9).

The reinforced concrete sample (RC) with 35mm cover and varying diameter of 12mm, 16mm, 20mm were designated as RC1, RC2, RC3 and with 45mm cover with similar diameter variation as RC4, RC5, RC6. Concrete mix with steel fiber with varying diameter for 35mm was designated SF1, SF2, SF3 and with 45mm cover as SF4, SF5, SF6. Concrete mix with steel fiber and ultrafine slag with 35mm was named as ASF1, ASF2, ASF3 and for 45mm ASF4, ASF5, ASF6 for 12mm, 16mm and 20mm diameter bars. Classification of specimen is shown in Table 3.6. A wooden end of size (100x100) mm were used to form support on the reinforcement protruding side. Holes in the wooden end allowed a single length of rebar to be suspended at a central location in the concrete beam (Figure 3.10). All the moulds were cleaned and oiled properly. Special care was taken to prevent form oil from contacting the reinforcing steel as this would be detrimental to the strength of the beam due to loss of bond strength that would be unrelated to corrosion damage. From the purchased lengths of reinforcement, the cleanest surfaces were selected for use in testing. These were securely tightened to correct dimensions before casting. Care was taken for the moulds so that there are no gaps left from where there is any possibility of leakage of plastic concrete. A careful procedure was adopted in the batching, mixing and casting operations (Figure 3.10). The coarse aggregates and fine aggregates were weighed first with an accuracy of 0.5 grams. PPC from single source was used in the whole process. Dry fine aggregates were introduced first in the mixer and mixed thoroughly. After that coarse aggregates were added to it. Then water was added carefully so that no water was loss during mixing. For addition of steel fiber in the respected samples the steel fiber was distributed randomly during mixing. Ultra fine slag was added after partial replacement of cement by 20%. The concrete mixture was prepared by the concrete mixer as well as with hand mixing. It was cleaned first by water and then dried to ensure any impurities were not adhering to its surface from prior to use. All the specimens were left in the steel mould for the first 24 hours at ambient condition. After that, they were de-moulded with care upon requirement of aging so that no edges were broken and were placed in the curing tank at the room temperature for curing. The room temperature for curing was 27 ± 20 as per IS: 10262-1982 [45] (Figure 3.11). Concrete must be properly cured to develop its optimum properties. To prevent evaporation of water from un-hydrated concrete, the specimens were immediately immersed in water for curing.

Table 3.6: Specimen classification

Specimen name	Diameter (mm)	Cover(mm)
RC1	12	35
RC2	16	35
RC3	20	35
RC4	12	45
RC5	16	45
RC6	20	45
SF1	12	35
SF2	16	35
SF3	20	35
SF4	12	45
SF5	16	45
SF6	20	45
ASF1	12	35
ASF2	16	35
ASF3	20	35
ASF4	12	45
ASF5	16	45
ASF6	20	45



Figure 3.8: Preparation of moulds



Figure 3.9: Random mixing of steel fiber



Figure 3.10: Casting of samples



Figure 3.11: Curing of samples.

3.6 PROCESSING IMPRESSED CURRENT METHOD

The impressed current technique, likewise called the galvanostatic technique, comprises of applying a steady current from a DC source to the steel inserted in concrete to initiate critical corrosion in a brief timeframe. After applying the current for a given length, the degree of initiated corrosion can be resolved hypothetically utilizing Faraday's law, or the level of real measure of steel lost in corrosion can be computed with the assistance of a gravimetric test led on the removed bars subsequent to subjecting them to quickened corrosion. Utilizing the genuine measure of steel lost in corrosion, an equal corrosion current density can be resolved.

3.6.1 Set-up used for inducing reinforcement corrosion through impressed current

Set-ups utilized for prompting reinforcement corrosion through impressed current comprise of a DC control source, a counter anode, and an electrolyte. The positive terminal of the DC control source is associated with the steel bars (anode) and the negative terminal is associated with the counter anode (cathode) (Figure 3.12). A current of 0.05 Ampere is inspired from counter anode to the rebars through concrete with the assistance of the electrolyte (ordinarily sodium chloride solution 3.5%). The power supplies had a current limit of 500 mill amperes in augmentations of 1 mA. The power supplies permit utilization of a steady current activity with programmed hybrid, which changes the non-constant parameters i.e. voltage or power, consequently to make the current constantly steady. These power supplies have a current precision of $\pm 1\%$ at 500 mA

full scale. The current intensity was selected in order to achieve the desired theoretical degree of corrosion of the steel within a certain time frame. Faraday's law was used to determine the theoretical mass loss.



Figure 3.12:DC voltage source

After curing, the specimen is immersed in 3.5% NaCl solution for 24 hours before testing for accelerated corrosion. The concrete specimens are immersed in a tank (Figure 3.13) such that water is below the top of concrete and not touching the reinforcement. After 24 hours specimens is introduced to accelerated corrosion process in the same tank by applying constant voltage (10V) until the development of first visible crack on the surface of specimen. A constant current density of 0.005 Ampere/sq.cm is induced with a built-in Multimeter to monitor the current. The water solution in the tank was changed after every 5 days. The direction of the current adjusted so that the reinforcing steel became an anode and the reference electrode as cathode, placed in the tank in sodium chloride solution that acted as electrolyte.



Figure 3.13 Impressed current set up.

CHAPTER 4

RESULTS AND DISCUSION

4.1 GENERAL

In this chapter after casting of desired samples, initiation of impressed current was done and degree of induced corrosion is calculated using Faraday's law. Difference between actual and theoretical mass loss was also calculated and then the results were tabulated in this chapter.

4.2 CALCULATIONS AND RESULTS

4.2.1 Degree of induced corrosion

The mass of rust produced per unit surface area of the bar due to applied current over a given time can be determined theoretically using the following expression based on Faraday's law [21]:

$$M_{th} = \frac{WI_{app}T}{F}$$

Where, M_{th} = theoretical mass of rust per unit surface area of the bar (g/cm^2); W = equivalent weight of steel which is taken as the ratio of atomic weight of iron to the valence of iron (27.925 g); I_{app} = applied current density (Amp/cm^2); T = duration of induced corrosion (sec); and F = Faraday's constant (96487 Amp-sec).

The actual mass of rust per unit surface area determined by gravimetric test on rebars extracted from the concrete by breaking the specimens after the accelerated corrosion test is completed:

$$M_{ac} = \frac{W_i - W_f}{\pi D L}$$

Where, M_{ac} = actual mass of rust per unit surface area of the bar (g/cm^2); W_i = initial weight of the bar before corrosion (g); W_f = weight after corrosion (g) for a given duration of induced corrosion (T); D = diameter of the rebar (cm); and L = length of the rebar sample (cm).

The degree of induced corrosion is also expressed in terms of the percentage weight loss (ρ) calculated as [21]:

$$\rho = \frac{W_i - W_f}{W_i} \times 100$$

The mass loss calculated by Faradays law is proportional to the current applied. The more the current the more is the mass loss.

4.2.2 Calculation of Induced corrosion

After the visibility of first surface crack on specimens, the steel reinforcing bars were retrieved, cleaned of rust, using stiff metal brush and then weighed to determine the actual mass loss of the steel bars (Figure 4.1). After removal of the concrete, it was clear that a concentration of corrosion was present in correspondence to both the crack location and the ends of the concrete specimens. The reinforcement used was measured before and after corrosion and measured by weighing machine. Later by using empirical formulas induced corrosion was calculated. Induced corrosion was calculated in Table 4.1 which varied maximum to 7.6% in terms of percentage of weight loss.



Figure 4.1: Corroded reinforcement

Table 4.1: Calculation of Degree of induced corrosion

Specimen	Dia. (cm) D	Length of bar (cm) L	Initial weight of bar (gm) W_i	Final weight of bar (gm) W_f	Time (s) T	Current (amp/cm ²) I_{app}	Loss (gm) ($W_i - W_f$)	Degree of induced corrosion (%) ρ
RC1	1.2	48	420	389	86400	0.005	31	7.381
RC2	1.6	48	680	658	103680	0.005	22	3.235
RC3	2.0	48	1100	1089	138960	0.005	11	1.000
RC4	1.2	48	420	394	95040	0.005	26	6.190
RC5	1.6	48	680	661	120960	0.005	19	2.794
RC6	2.0	48	1100	1093	129600	0.005	7	0.636
SF1	1.2	48	420	409	972000	0.005	11	2.619
SF2	1.6	48	680	669	1042560	0.005	11	1.618
SF3	2.0	48	1100	1087	1274400	0.005	13	1.182
SF4	1.2	48	420	411	975600	0.005	9	2.143
SF5	1.6	48	680	671	1044000	0.005	9	1.324
SF6	2.0	48	1100	1095	1296000	0.005	5	0.455
ASF1	1.2	48	420	416	993600	0.005	4	0.952
ASF2	1.6	48	680	678	1123200	0.005	2	0.294
ASF3	2.0	48	1100	1098	1296000	0.005	2	0.182
ASF4	1.2	48	420	418	1123200	0.005	2	0.476
ASF5	1.6	48	680	679.5	1728000	0.005	0.5	0.074
ASF6	2.0	48	1100	1099.6	2073600	0.005	0.4	0.036

4.2.3 Comparison of Actual mass loss and Theoretical mass loss

This actual mass loss (M_{ac}) of steel bars is compared with the theoretical mass loss (M_{th}) calculated by Faraday's law given in Table 4.2 and the corresponding graphical representation in Figure 4.2. Which shows that the actual value resulted are a bit higher than the theoretical values, which certainly does fulfill the theoretical criteria. This also resulted because some time is required for depassivation of the steel bar.

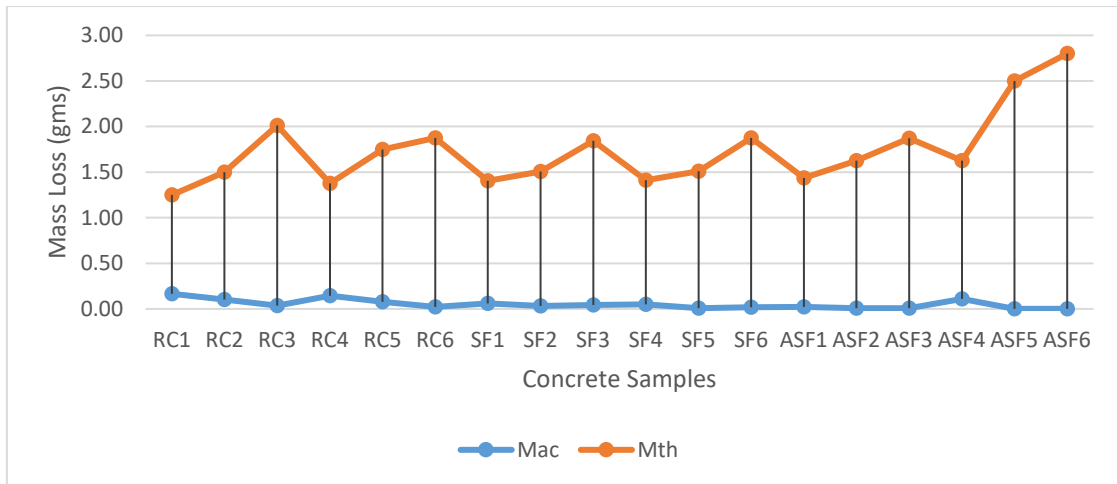


Figure 4.2: Comparison of Actual mass loss and Theoretical mass loss

Table 4.2: Comparison of actual mass loss (M_{ac}) of steel bars with the theoretical mass loss (M_{th}).

Specimen	Diameter (mm)	M_{ac} (gm/cm sq.)	M_{th} (gm/cm sq.)
RC1	12	0.171	1.250
RC2	16	0.091	1.500
RC3	20	0.036	2.011
RC4	12	0.144	1.375
RC5	16	0.079	1.750
RC6	20	0.023	1.875
SF1	12	0.061	1.406
SF2	16	0.046	1.508
SF3	20	0.043	1.844
SF4	12	0.050	1.412
SF5	16	0.037	1.511
SF6	20	0.017	1.875
ASF1	12	0.022	1.438
ASF2	16	0.008	1.625

ASF3	20	0.007	1.875
ASF4	12	0.011	1.625
ASF5	16	0.0021	2.500
ASF6	20	0.0013	3.000

4.2.4 Effect of cover depth on actual mass loss

It was observed that for various cover depth the mass loss also varied along with variation in the bar diameter. The maximum mass loss was in the bar with minimum diameter of 12mm and decreasing linearly with increasing diameter (Figure 4.3). As the cover depth increased the mass loss decreased in the two set of cover depth samples i.e. 35mm and 45mm. As the cover increased the corrosion mass loss decreased.

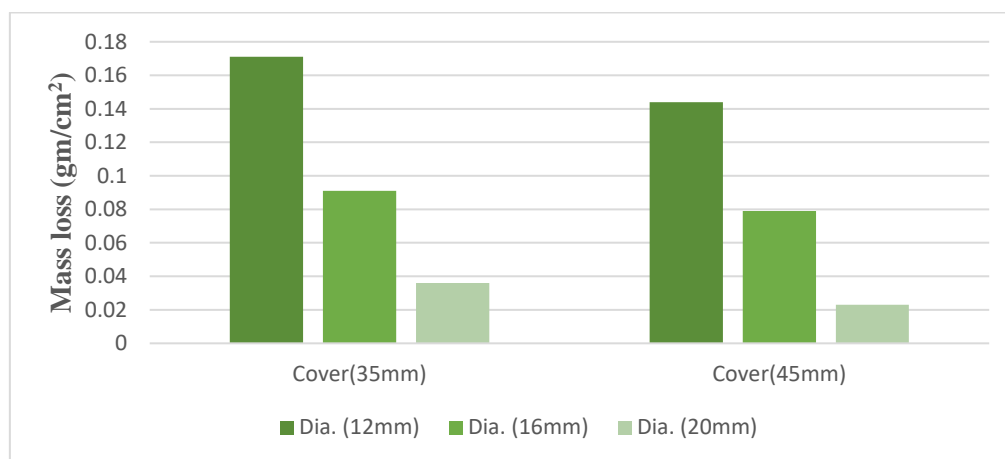


Figure 4.3: Variation of Actual mass (M_{ac}) for different cover depths in RCC beams.

In steel fiber reinforced concrete, there is very little mass loss in the bar with the highest diameter with maximum mass loss in 12mm diameter bar (Figure 4.5). In terms of cover, there was a slight more mass loss in 35mm cover samples than the 45mm ones. Time required for the development of first visible crack on the surface of concrete sample increased slightly as the cover increased. It could be seen that the samples containing steel fiber in the mix staining due to corroded steel fibers on the surface of (Figure 4.4).



Figure 4.4: Staining due to steel fiber corrosion.

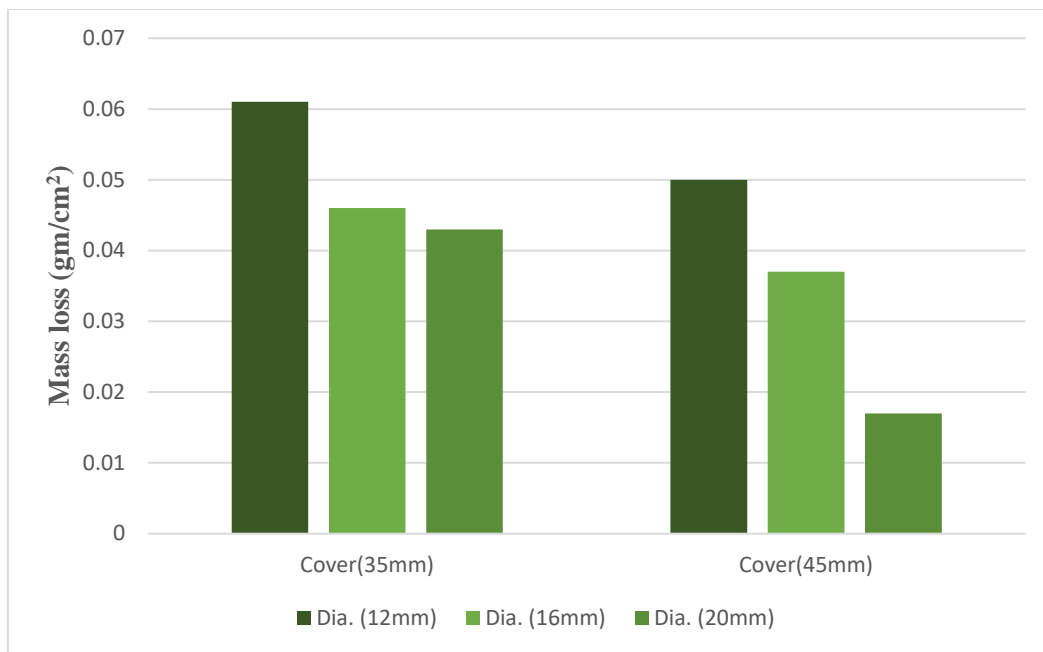


Figure 4.5: Variation of Actual mass (M_{ac}) for different cover depths in Steel fiber reinforced concrete beams.

After the addition of ultrafine slag and steel fiber in concrete mix, the mass loss decreased in the bar with higher diameter as almost there was little mass loss (Figure 4.6). The samples with more cover depth showed less corrosion.

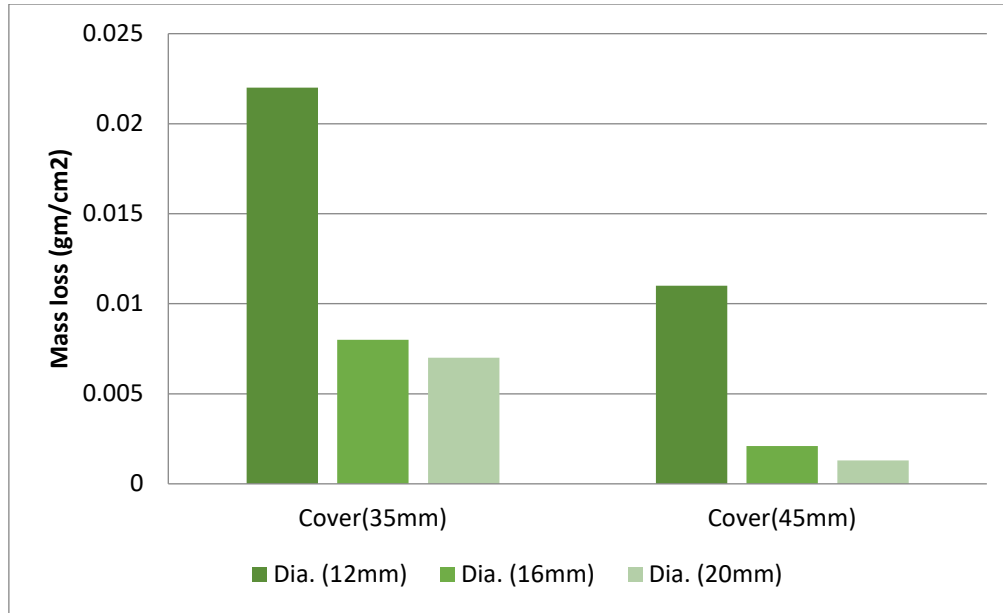


Figure 4.6: Variation of Actual mass (M_{ac}) for different cover depths in Steel fiber reinforced concrete along with ultra-fine slag beams.

4.2.5 Flexural strength of corroded and non-corroded samples

The testing machine is of adequate limit with respect to the tests and equipped for applying the load at the rate to such an extent that the outrageous fiber push increments at roughly 7 $kg/cm^2/min$. The rate of loading is 400 kg/min for the 15 cm specimens and a rate of 180 kg/min for the 10 cm specimens. The load might be expanded until the point when the specimen falls flat, and the greatest load connected to the specimen amid the test should be recorded. The presence of the broken appearances of concrete and any surprising highlights or sort of disappointment should be noted. The passable mistakes might be not more noteworthy than ± 0.5 percent of the connected load where a high level of exactness is required and not more noteworthy than ± 1.5 percent of the connected load for business sort of utilization. The bed of the testing machine is furnished with two steel rollers, 38 mm in measurement, on which the specimen is to place and these rollers might be mounted to the point that the separation from center to center is 60 cm for 15.0 cm specimens or 40 cm for 10.0 cm specimens The load might be connected through two comparable rollers mounted at the third purposes of the supporting traverse that is, divided at 20 or 13.3 cm center to center. The load might be distributed similarly between the two loading rollers, and all rollers should be mounted in such a way, to the point that the load is connected pivotally and without subjecting the specimen to any torsional stresses

or restrains. One appropriate arrangement which follows these prerequisites is demonstrated in (Figure 4.7)



Figure 4.7: Flexure testing of corroded samples

The flexural strength of the specimen is expressed as the modulus of rupture f_b ,

$$f_b = \frac{3FL}{2bd^2}$$

Where F= is the axial load at the fracture, b= width, d= depth or thickness of material and L = length of the support span.

Table 4.3: Comparison of flexural strength of corrode and non-corroded bars.

Sr. No.	Specimens	Reinforcement diameter (mm)	Cover depth (mm)	Flexural strength of non-corroded specimen(N\mm ²)	Flexural strength of corroded specimen(N\mm ²)
1.	RC1	12	35	21.51	18.00
2.	RC2	16	35	24.62	17.01
3.	RC3	20	35	29.88	19.44
4.	RC4	12	45	21.20	18.90
5.	RC5	16	45	23.85	20.56
6.	RC6	20	45	29.26	25.65
7.	SF1	12	35	25.01	20.02
8.	SF2	16	35	25.89	21.38
9.	SF3	20	35	30.50	21.87
10.	SF4	12	45	25.96	24.66
11.	SF5	16	45	31.78	25.29
12.	SF6	20	45	34.80	25.79
13.	ASF1	12	35	31.64	29.03

14.	ASF2	16	35	34.68	29.57
15.	ASF3	20	35	42.85	30.60
16.	ASF4	12	45	30.47	24.93
17.	ASF5	16	45	39.14	29.50
18.	ASF6	20	45	51.89	31.56

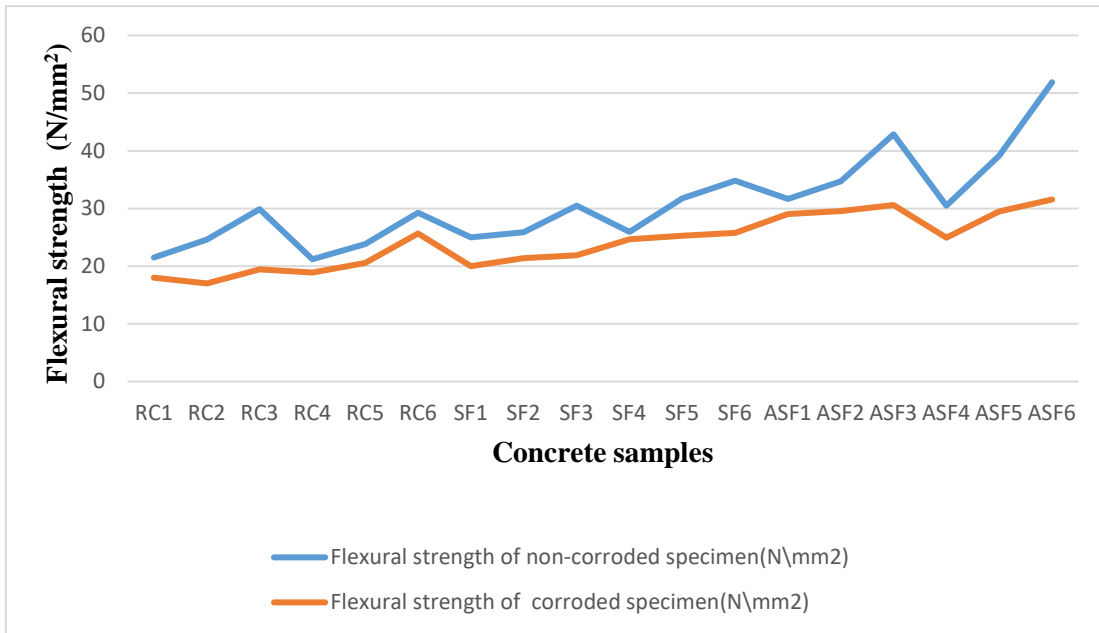


Figure 4.8: Comparison of flexure strength of corroded and non-corroded specimen

The cover depth, when increased provides resistance against corrosion, and hence preserves the flexural strength of beam after corrosion. The overall corroded specimens are showing decrease in strength as the corrosive products decrease the strength due to mass loss of the bar and even by onsets of crack propagation as shown in Table 4.3 and Figure 4.8.

4.2.6 Depth of penetration of corrosion

By means of the accelerated corrosion method, the steel bar can be treated to attain a certain level of corrosion. The degree of corrosion or corrosion level was measured as the loss in weight of the steel bar relative to the weight of unit length before corroding. To calculate the corrosion depth, the following equation (Eq. 2.1) was used [10]:

$$d = s \times d_b / 4 \text{-----Eq. 2.1}$$

Where, d = the corrosion depth (mm); s = Loss of bar/Original weight of bar (grams); d_b = diameter of steel bar(mm)

The depth of penetration calculated is shown in Table 4.4. The corresponding pictures shows the corrosion depths in (Figure 4.9).

Table 4.4: Depth of Penetration of corrosion in the concrete samples

Specimen	Diameter of bar (mm) d_b	Initial weight of bar (W_i)	Final weight of bar (W_f)	Loss(gm)	Loss of bar/Original weight of bar (s)	Depth of penetration (mm)
RC1	12	420	390	31	0.074	0.221
RC2	16	680	655	22	0.032	0.129
RC3	20	1100	1086	11	0.010	0.050
RC4	12	420	362	26	0.062	0.186
RC5	16	680	633	19	0.028	0.112
RC6	20	1100	1089	7	0.006	0.032
SF1	12	420	409	11	0.026	0.079
SF2	16	680	669	11	0.016	0.065
SF3	20	1100	1087	13	0.012	0.059
SF4	12	420	411	9	0.021	0.064
SF5	16	680	671	9	0.013	0.053
SF6	20	1100	1095	5	0.005	0.023
ASF1	12	420	416	4	0.010	0.029
ASF2	16	680	678	2	0.003	0.012
ASF3	20	1100	1098	2	0.002	0.009
ASF4	12	420	418	2	0.005	0.014
ASF5	16	680	679.5	0.5	0.001	0.003
ASF6	20	1100	1099.6	0.4	0.000	0.002



Figure 4.9: Corrosion depth of the concrete samples

This implies that the trend followed by corrosion penetration has decreased by addition of steel fiber and ultra fine additive. The bar with larger diameter seems to create less corrosion depth by addition of fiber and admixtures therefore, a large bar needs a longer duration for producing a similar corrosion level.

CHAPTER 5

CONCLUSIONS AND RECOMMENDATIONS

5.1 CONCLUSION

As we know that corrosion is the main problem that is being faced. Detailed laboratory work was performed on different types of reinforced concrete samples by variations which concluded to the following results:

- According to the accelerated corrosion method adopted in this research, large steel bars need longer duration, compared for producing a similar corrosion level, but tend to exhibit high corrosion depth.
- The variation in clear cover on the sample produced a little effect on corrosion, as it took almost similar time to induce corrosion in the samples.
- The reinforced concrete samples showed less time to corrode than the ones with extra additives.
- Mix of ultra-fine slag and steel fiber samples of concrete showed approximately 2 percent less corrosion than the steel fiber reinforced concrete and approximately 7.6 percent more than normal reinforced concrete sample.

5.2 FUTURE SCOPE

- This work can be further extended to study the microstructural analysis of corrosion in steel bars.
- Life cycle assessment of the concrete structure can also be defined by actual experimental setups.

REFERENCES

- [1] Chakravarthy, P.R. K., and Raj, R.R. (2017). “Analysis on Compressive Strength of Concrete with partial replacement of Cement with Alccofine.” *ARPJ Journal of Engineering and Applied Science*, 12(8), 2392-2395.
- [2] Parvatareddy, S.B., and Naidu, G.G. (2017). “Comparative Study on Various Methods Used for Corrosion Protection of Rebar in Concrete.” *International Journal of Scientific Engineering and Technology Research*, 6 (8), 1522-1527.
- [3] Kim, B.J., and Yi, C. (2017). “Effect of embedment length on pullout behavior of amorphous steel fiber in Portland cement composites.” *Construction and Building Materials*, 143(1), 83-91.
- [4] Alizade, E., Alaei, F.J., and Zabihi, S. (2016). “Effect of Steel Fiber Corrosion on Mechanical properties of Steel Fiber Reinforced Concrete.” *Asian Journal of Civil Engineering*, 17(2), 147-158.
- [5] Liu, M., Cheng, X., Li, X., Hu, J., Pan, Y., and Jin, Z. (2016). “Indoor accelerated corrosion test and marine field test of corrosion-resistant low-alloy steel rebars.” *Case Studies in Construction Materials*.
- [6] Altoubat, S., Maalej, M., and Shaikh, F.U.A. (2016). “Laboratory Simulation of Corrosion Damage in Reinforced Concrete.” *International Journal of Concrete Structures and Materials*, 10(3), 383–391.
- [7] Behera, P.K., Moon, A.P.K., Mondal, K., and Misra, S. (2016). “Estimating critical corrosion for initiation of longitudinal cracks in RC structures considering phases and composition of corrosion products.” *Journal of Materials in Civil Engineering*, 28(12), 0401615/ 1-04016158/12.
- [8] Huo, S. (2016). “Modeling corrosion-induced cracking in reinforced concrete”, *University of Glasgow*, 1(1).
- [9] Rathod, N.G.S.M., and Moharana, N.C. (2015). “Advanced methods of corrosion monitoring - A Review.” *International Journal of Research in Engineering and Technology*, 4(1), 413-420.

- [10] Huang, C.H. (2014). "Effects of rust and scale of reinforcing bars on the bond performance of reinforcement concrete." *Journal of Materials in Civil Engineering*, 26(4), 5, 76-581.
- [11] Kumar, V., Singh, R., and Quraishi, M. A. (2013). "A Study on Corrosion of Reinforcement in Concrete and Effect of Inhibitor on Service Life of RCC." *Journal of Materials and Environmental Science*, 4 (5), 726-731.
- [12] Pouya1, H.S., Ganjian, E., Claisse, P., and Muthuramalingam, K. (2013). "Corrosion durability of high performance steel fibre reinforced concrete." *Third International Conference on Sustainable Construction Materials and Technologies*.
- [13] Rao, K.S., Kumar, S.R., and Narayana, A.L. (2013). "Comparison of Performance of Standard Concrete And Fiber Reinforced Standard Concrete Exposed To Elevated Temperatures." *American Journal of Engineering Research*, 2(3), 20-26.
- [14] Solgaard, A.O.S., Michel, A., Geiker, M., and Stang, H. (2013). "Concrete cover cracking due to uniform reinforcement Corrosion." *Materials and Structures*, 46 (11), 1781-1799.
- [15] Poursaee, A. (2011). "Corrosion Measurement Techniques in Steel Reinforced Concrete." *Journal of ASTM International*, 8 (5), 1-15.
- [16] Mihashi, H., Ahmed, S.F.U., and Kobayakawa, A. (2011). "Corrosion of Reinforcing Steel in Fiber Reinforced Cementitious Composites." *Journal of Advanced Concrete Technology*, 9(2), 159-167.
- [17] Balouch, S.U., Forth, J.P., and Granju, J.L. (2010). "Surface corrosion of steel fibre reinforced concrete." *Cement and Concrete Research*, 40 (1), 410-414.
- [18] Lu, C.H., Liu, R.G., and Jin, W.L. (2010). "A model for predicting time to corrosion-induced cover cracking in reinforced concrete structures." *Fracture Mechanics of Concrete and Concrete Structures -Assessment, Durability, Monitoring and Retrofitting of Concrete Structures*, 967-975.
- [19] Dimitri, V.V., Chernin, L., and Stewart, M.G. (2009). "Experimental and numerical investigation of corrosion-induced cover cracking in reinforced concrete structures." *Journal of Structural Engineering*, 135(4), 376 -385.

- [20] Lee, H.S. and Cho, Y.S. (2009). "Evaluation of the mechanical properties of steel reinforcement embedded in concrete specimen as a function of the degree of reinforcement corrosion." *International Journal of Fracture*, 157(1), 81–88.
- [21] Ahmad, S. (2009). "Techniques for inducing accelerated corrosion of steel in concrete." *The Arabian Journal for Science and Engineering*, 95–104.
- [22] Care, S., and Raharinaivo, A. (2007). "Influence of impressed current on the initiation of damage in reinforced mortar due to corrosion of embedded steel." *Cement and Concrete Research*, 37 (1), 1598–1612.
- [23] Yingshu, Y., Yongsheng, J., and Shah, S.P. (2007). "Comparison of Two Accelerated Corrosion Techniques for Concrete Structures." *ACI Structural Journal*, (104), 344–347.
- [24] Poursaei, A.E. (2007). "An Analysis of the Factors Influencing Electrochemical Measurements of the Condition of Reinforcing Steel in Concrete Structures." *University of Waterloo, Waterloo Ontario, Canada*.
- [25] Smith, R. (2007). "The effects of corrosion on the performance of reinforced concrete beams." Theses and dissertations.
- [26] Ormellese, M., Berra, M., Bolzoni, F., and Pastore, T. (2006). "Corrosion inhibitors for chlorides induced corrosion in reinforced concrete structures." *Cement and Concrete Research*, 36 (3), 536–547.
- [27] Leelalerkiet, V., Kyung, J., Ohtsu, M., and Yokota, M. (2004). "Analysis of half-cell potential measurement for corrosion of reinforced concrete." *Construction and Building Materials*, 18 (1), 155–162.
- [28] Elsener, B., Andrade, C., Gulikers, J., Polder, R., and Raupach, M. (2003). "Half-cell potential measurements—Potential mapping on reinforced concrete structures." *Material and Structure*, (36), 461–471.
- [29] Tamer, A., Maaddawy, E., and Khaled, A.S. (2003), "Effectiveness of Impressed Current Technique to Simulate Corrosion of Steel Reinforcement in Concrete." *Journal of Materials in Civil Engineering*, 15(1), 41- 47.
- [30] Ramachandran, S., Campbell, S., and Ward, M.B. (2001). "The Interactions and Properties of Corrosion Inhibitors with Byproduct Layers." *NACE International* (57).26-31.

- [31] Ahn, W. (2001). "Galvanostatic testing for the durability of marine concrete under fatigue loading." *Cement and Concrete Research*, (31), 343–349.
- [32] Alonsol, C., Andydel, C., Rodyigtrez, J., and Diex, J. M. (1998). "Factors controlling cracking of concrete affected by reinforcement corrosion." *Material and structures*, 31(1), 435-441.
- [33] Ohtsu, M., and Yosimura, S. (1997). "Analysis of crack propagation and crack initiation due to corrosion of reinforcement." *Construction and Building Materials*, 11 (7–8), 437–442.
- [34] Suda, K., Misra, S., and Motohash, K. (1993). "Corrosion products of reinforcing bars embedded in concrete." *Corrosion science*, 35(1), 1543-1549.
- [35] Leek, D.S. (1991). "The passivity of steel in concrete." *Quarterly Journal of Engineering Geology*, 24(1), 55-66.
- [36] Tuutti, K. (1982). "Corrosion of steel in concrete." *Swedish Cement and Concrete Research Institute, Stockholm*.
- [37] ISO 8044:2015, "Corrosion of Metals and Alloys- Basic Terms and Definitions."
- [38] IS 456:2000, "Plain and Reinforced Concrete - Code of Practice", *Bureau Indian Standard*, New Delhi, India.
- [39] IS 9077:1979, "Indian Standard- Code of Practice for Corrosion Protection of Steel Reinforcement in RB and RCC Construction." *Indian Standards Institution*, New Delhi, India.
- [40] IS 383: 1970, "Indian standard Specifications for coarse and fine aggregates from natural sources for Concrete." *Bureau of Indian Standards*, New Delhi, India.
- [41] IS 2386(Part 1):1963, "Methods of test for aggregates for concrete: Part 1 Particle size and shape." *Bureau of Indian Standards*, New Delhi, India.
- [42] IS 4031: Part 4: 1988, "Methods of physical tests for hydraulic cement: Part 4 Determination of consistency of standard cement paste." *Bureau of Indian Standards*, New Delhi, India.
- [43] IS 4031: Part 5: 1988, "Methods of physical tests for hydraulic cement: Part 5 Determination of initial and final setting time." *Bureau of Indian Standards*, New Delhi, India.

- [44] IS 4031: Part 11: 1988, "Methods of physical tests for hydraulic cement: Part 11 Determination of density." *Bureau of Indian Standards*, New Delhi, India.
- [45] IS 10262: 1982, "Recommended guidelines for concrete mix design" *Bureau of Indian Standards*, New Delhi, India
- [46] <http://corrosion-doctors.org/Principles/Course.htm>
- [47] Revie, W., and Uhlig, H.H. (2007). "Corrosion and Corrosion Control an Introduction to Corrosion Science and Engineering." *John Wiley & Sons, Inc.* 4(1).
- [48] Broomfield, J.P. (2007). "Corrosion of Steel in Concrete: Understanding, Investigation and Repair." *Taylor & Francis*.
- [49] Shetty, M.S. (2005). "Concrete Technology-Theory and Practice." S. Chand and Co.
- [50] Santhakumar, A.R. (2007). "Concrete Technology." *Oxford University Press*.
- [51] Sohail, M.G. (2013). "Corrosion of steel in concrete Development of an Accelerated Test by Carbonation and Galvanic Coupling." *University Toulouse III-Paul Sabatier*.
- [52] Chanh, N., V. "Steel Fiber Reinforced Concrete." *Research note, Ho Chi Minh City University of Technology*, (108-116).

**JAYPEE UNIVERSITY OF INFORMATION TECHNOLOGY, WAKNAGHAT
LEARNING RESOURCE CENTER**

PLAGIARISM VERIFICATION REPORT

Date: 10/05/18

Type of Document (Tick): Thesis M.Tech Dissertation/ Report B.Tech Project Report Paper

Name: NIMISHA SHARMA Department: CIVIL ENGINEERING

Enrolment No. 162654 Registration No. _____

Phone No. 9418129172 Email ID. nimishas101@gmail.com

Name of the Supervisor: DR. SAURAV

Title of the Thesis/Dissertation/Project Report/Paper (In Capital letters): THE EFFECTS OF CORROSION IN REINFORCED CONCRETE WITH ADDITION OF STEEL FIBER AND MINERAL ADMIXTURE

Kindly allow me to avail Turnitin software report for the document mentioned above.

Nimishka
(Signature)

FOR ACCOUNTS DEPARTMENT:

Amount deposited: Rs. 500/- Dated: 10/5/18 Receipt No. B/R 1805/289
(Enclosed payment slip)

[Signature]
(Account Officer)

FOR LRC USE:

The above document was scanned for plagiarism check. The outcome of the same is reported below:

Copy Received on	Report delivered on	Similarity Index in %	Submission Details	
			Word Counts	Character Counts
10/05/2018	11/05/2018	16%	17,098	86,814
			Page counts	69
			File Size	2.65M

Checked by [Signature]
Name & Signature

Librarian
[Signature]
LIBRARIAN
LEARNING RESOURCE CENTER
Jaypee University of Information Technology
Waknaghat, Distt, Solan (Himachal Pradesh)



Digital Receipt

This receipt acknowledges that Turnitin received your paper. Below you will find the receipt information regarding your submission.

The first page of your submissions is displayed below.

Submission author: Nimisha Sharma
Assignment title: MTech Project Reports
Submission title: THE EFFECTS OF CORROSION IN...
File name: M.Tech_Nimisha_162654.pdf
File size: 2.65M
Page count: 69
Word count: 17,098
Character count: 86,814
Submission date: 11-May-2018 10:53AM (UTC+0530)
Submission ID: 962267816

THE EFFECTS OF CORROSION IN
REINFORCED CONCRETE WITH ADDITION OF STEEL
FIBER AND MINERAL ADMIXTURE

A Thesis
submitted in partial fulfillment of the requirements for the award of the degree

of
MASTER OF TECHNOLOGY

IN

CIVIL ENGINEERING

With specialization in

STRUCTURAL ENGINEERING

Under the
supervision of

DR. SAURAV
(ASSISTANT PROFESSOR)

by

NIMISHA SHARMA
(162654)



JAYPEE UNIVERSITY OF INFORMATION TECHNOLOGY,

WAKNAGHAT, SOLAN-173234

HIMACHAL PRADESH, INDIA

(MAY-2018)

LIBRARY
LEARNING RESOURCE CENTER

Jaypee University of Information Technology
Waknaghat, Distt. Solan (Himachal Pradesh)
Pin Code: 173234